JOURNAL OF PETROLOGY | VOLUME 46 | NUMBER 4 | PAGES 829–858 | 2005 | doi:10.1093/petrology/egi002

Evidence for a Widespread Tethyan Upper Mantle with Indian-Ocean-Type Isotopic Characteristics

S.-Q. ZHANG[1], J. J. MAHONEY[1]*, X.-X. MO[2], A. M. GHAZI[3], L. MILANI[1,4], A. J. CRAWFORD[5], T.-Y. GUO[2] AND Z.-D. ZHAO[2]

[1]SCHOOL OF OCEAN AND EARTH SCIENCE AND TECHNOLOGY, UNIVERSITY OF HAWAII, HONOLULU, HI 96822, USA

[2]CHINA UNIVERSITY OF GEOSCIENCES, BEIJING 100083, P. R. CHINA

[3]GEOLOGY DEPARTMENT, GEORGIA STATE UNIVERSITY, ATLANTA, GA 30303, USA

[4]INSTITUTE OF MINERALOGY, UNIVERSITY OF FERRARA, 44100 FERRARA, ITALY

[5]CENTRE FOR ORE DEPOSIT STUDIES, UNIVERSITY OF TASMANIA, HOBART, TAS. 7001, AUSTRALIA

RECEIVED APRIL 21, 2004; ACCEPTED NOVEMBER 23, 2004
ADVANCE ACCESS PUBLICATION JANUARY 21, 2005

The mantle sources of Tethyan basalts and gabbros from Iran, Tibet, the eastern Himalayas, the seafloor off Australia, and possibly Albania were isotopically similar to those of present-day Indian Ocean ridges and hotspots. Alteration-resistant incompatible element compositions of many samples resemble those of ocean-ridge basalts, although ocean-island-like compositions are also present. Indian-Ocean-type mantle was widespread beneath the Neotethys in the Jurassic and Early Cretaceous, and present beneath at least parts of the Paleotethys as long ago as the Early Carboniferous. The mantle beneath the Indian Ocean today thus may be largely 'inherited' Tethyan mantle. Although some of the Tethyan rocks may have formed in intra-oceanic back-arcs or fore-arcs, contamination of the asthenosphere by material subducted shortly before magmatism cannot be a general explanation for their Indian-Ocean-ridge-like low-$^{206}Pb/^{204}Pb$ signatures. Supply of low-$^{206}Pb/^{204}Pb$ material to the asthenosphere via plumes is not supported by either present-day Indian Ocean hotspots or the ocean-island-like Tethyan rocks. Old continental lower crust or lithospheric mantle, including accreted, little-dehydrated marine sedimentary material, provides a potential low-$^{206}Pb/^{204}Pb$ reservoir only if sufficient amounts of such material can be introduced into the asthenosphere over time. Anciently subducted marine sediment is a possible low-$^{206}Pb/^{204}Pb$ source only if the large increase of U/Pb that occurs during subduction-related dewatering is somehow avoided. Fluxing of low-U/Pb fluids directly into the asthenosphere during ancient dewatering and introduction of ancient pyroxenitic lower-crustal restite or basaltic lower-arc crust into the asthenosphere provide two other means of creating Tethyan–Indian Ocean mantle, but these mechanisms, too, have potentially significant problems.

KEY WORDS: *Indian Ocean; mantle geochemical domains; ophiolites; Tethyan Ocean*

INTRODUCTION

The origin of the vast Indian Ocean mantle domain is unknown. This domain stretches from south of Australia along the Southeast Indian Ridge (Klein *et al.*, 1988; Pyle *et al.*, 1992) to south of Africa on the Southwest Indian Ridge (Mahoney *et al.*, 1992), northward along the Central Indian and Carlsberg ridges, and into the Red Sea (Volker *et al.*, 1993). Basalts formed along these ridges are characterized by lower $^{206}Pb/^{204}Pb$ relative to ε_{Nd}, $^{208}Pb/^{204}Pb$, and $^{207}Pb/^{204}Pb$ than the great majority (>95%) of Pacific and North Atlantic mid-ocean ridge basalts (MORB), and tend to have comparatively high $^{87}Sr/^{86}Sr$ and low ε_{Nd} (e.g. Subbarao & Hedge, 1973; Hedge *et al.*, 1979; Dupre & Allègre, 1983; Hamelin *et al.*, 1986; Michard *et al.*, 1986; Price *et al.*, 1986; Dosso *et al.*, 1988; Mahoney *et al.*, 1989, 2002; Rekhkämper & Hofmann, 1997). Ocean-island basalts (OIB) in the Indian Ocean exhibit qualitatively similar Pb–Nd–Sr isotopic characteristics (e.g. Hart, 1988) but have higher $^{206}Pb/^{204}Pb$ than most Indian MORB. Isotopically

*Corresponding author. Telephone: 808-956-8705. Fax: 808-956-5512. Email: jmahoney@hawaii.edu

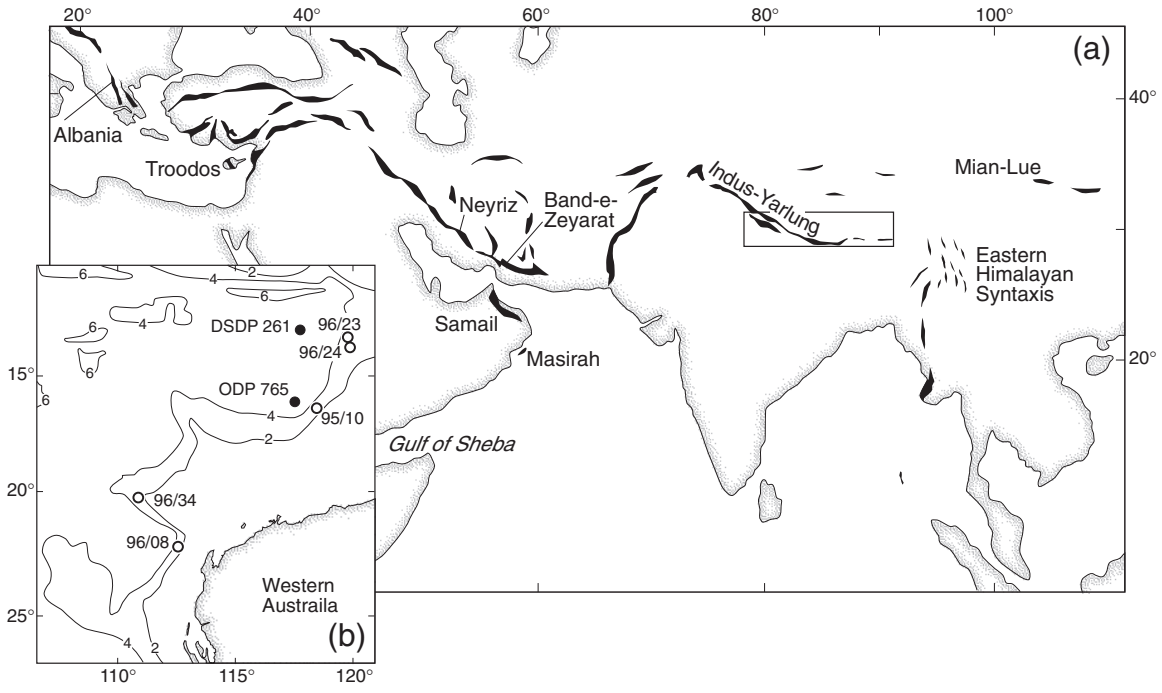

Fig. 1. (a) Map indicating the principal Tethyan ophiolite and mélange zones in black (after Coleman, 1981); locations discussed in the text are labeled and the area detailed in Fig. 2 is indicated. (b) Northwestern Australian margin, with locations of dredge and drill sites studied (after Crawford & von Rad, 1994). Numbers on depth contours are in kilometers.

Indian-MORB-like mantle also feeds part of the Southern Mid-Atlantic Ridge (e.g. Hanan *et al.*, 1986; Douglass *et al.*, 1999; Kamenetsky *et al.*, 2001) and broadly similar isotopic signatures are characteristic of several marginal basins and island arcs in the Western Pacific (e.g. Mukasa *et al.*, 1987; Stern *et al.*, 1993; Crawford *et al.*, 1995; Hickey-Vargas *et al.*, 1995; Castillo, 1996; Spadea *et al.*, 1996; Hickey-Vargas, 1998).

Information on the history of this mantle domain is provided by basalts from drill and dredge sites on old Indian Ocean seafloor (Lanyon, 1995; Pyle *et al.*, 1995; Weis & Frey, 1996; Mahoney *et al.*, 1998). Isotopic data for such sites show that mantle similar to that beneath the modern Indian Ocean was present, at least in places, as long ago as 140 Ma, the age of the oldest true Indian Ocean crust yet sampled. Additional information on the history of this domain may be provided by remnants of Tethyan seafloor, because the now-vanished Tethyan Ocean covered much of the same geographical region currently occupied by the Indian Ocean, which began opening at around 160 Ma (e.g. Lawver & Gahagan, 1993; Lawver *et al.*, 2000; Stampfli & Borel, 2002). Although Tethyan seafloor has been largely subducted, a small portion remains intact off northwestern Australia, and fragments of both Neotethyan (primarily Jurassic and Cretaceous) and Paleotethyan (primarily pre-Triassic) lithosphere are preserved in ophiolites and mélanges along the Tethyan suture zones of Eurasia (Fig. 1).

Reconnaissance study of Early Cretaceous (~120 Ma) Neotethyan basalts in the Xigaze ophiolite of Tibet has revealed strongly Indian-MORB-type Nd–Pb isotopic characteristics (Mahoney *et al.*, 1998). The Nd–Pb isotopic signatures of Neotethyan rocks of the middle Cretaceous Samail ophiolite of Oman (Chen & Pallister, 1981; McCulloch *et al.*, 1981; Benoit, 1997) also point to an isotopically Indian-Ocean-type mantle source. However, Late Jurassic MORB-type basalts and gabbros of the Masirah ophiolite of Oman, which represents 150 Ma oceanic lithosphere formed near the boundary between the southern Neotethys and the nascent Indian Ocean, lack clear Indian-MORB-type characteristics (Mahoney *et al.*, 1998). Data for Neotethyan MORB of similar age at Deep Sea Drilling Project (DSDP) Site 261 off northwestern Australia indicated that those rocks also lack an Indian-MORB-type signature (Weis & Frey, 1996). On the basis of these results, Mahoney *et al.* (1998) suggested that the Indian Ocean mantle domain may pre-date the ~160 Ma opening of the Indian Ocean by only a few tens of millions of years, and speculated that asthenosphere from beneath the young Indian Ocean may have flowed into the Tethyan region in the Early Cretaceous. An even younger origin for the Indian Ocean mantle domain was proposed by Weis & Frey (1996), who linked it to the appearance of the Kerguelen hotspot, now estimated at ~120 Ma (Duncan, 2002). In contrast, the possibility of a much older origin for

this mantle domain is suggested by Nd and Pb isotopic data for the Paleotethyan Mian–Lue northern ophiolite of central China and the Jinsha River and Shuanggou ophiolites of southwestern China, which display age-corrected values in or rather close to the range expected for Indian MORB mantle at 350 Ma (Xu *et al.*, 2002; Xu & Castillo, 2004). However, indications of disturbance to the Pb isotope system, such as high $(^{207}Pb/^{204}Pb)_t$ values (where the subscript t indicates age-corrected) and anomalously high Pb concentrations, were present in some of the samples.

Here, we report age-corrected Nd–Pb–Sr isotope data for ~100–350 Ma basalt, diabase, and gabbro from widely separated Tethyan locations in Tibet, Iran, Albania, the eastern Himalayan syntaxis, and the seafloor off NW Australia (Fig. 1). Our results indicate that isotopically Indian-Ocean-type mantle underlay much of the Neotethys in the Jurassic and Early Cretaceous, and support its presence below at least part of the Paleotethys as long ago as the Early Carboniferous.

METHODS AND SAMPLES

All of the rocks have been affected by seawater-mediated alteration, although to variable extents and under a range of temperature and pressure, from clay-forming conditions to upper greenschist facies (Girardeau *et al.*, 1985; Beccaluva *et al.*, 1994; Crawford & von Rad, 1994; Mo *et al.*, 1994, 1998; Hassanipak *et al.*, 1996; Bortolotti *et al.*, 2002; Shen *et al.*, 2002*a*, 2002*b*; Zhou *et al.*, 2002; Ghosh & Ray, 2003; Ghazi *et al.*, 2004). In this respect the samples are very similar to the Tethyan rocks studied by Mahoney *et al.* (1998), and we employed identical sample preparation and analytical procedures. A critical first step is careful sample selection, followed by hand-picking of small chips under a stereomicroscope (rejecting samples or parts of sample with visible phosphate, ferromanganese oxide, sulfide, or carbonate, areas with veins, vesicle fillings, etc.). For age-correcting isotope ratios, concentrations of Sm, Nd, U, Th, Pb, Rb, and Sr were measured by isotope dilution on the same dissolution of hand-picked, acid-cleaned (5 min in 0·1 M HF + HNO_3 in an ultrasonic bath) rock chips and, in some cases, strongly acid-leached powder, as that analyzed for Nd, Sr, and Pb isotopes (Tables 1 and 2). Because the preparation procedure tends to modify a sample's mineralogical composition relative to that of the bulk rock, the isotope-dilution concentrations generally cannot be taken to represent whole-rock values, particularly for coarser-grained or more altered samples. Whole-rock incompatible trace-element concentrations were determined for a subset of previously unanalyzed samples by inductively coupled plasma–mass spectrometry (Table 3). For major element and additional trace element data, we refer the reader to the references cited in the relevant sections below. A set of published major and trace element data is available for downloading from the *Journal of Petrology* website at http://www.petrology.oupjournals.org (Electronic Appendices 1 and 2).

Because of alteration, age-corrected Sr isotope ratios generally cannot be assumed to represent magmatic values. Similarly, concentrations of Rb, U, and Ba have been modified substantially in many cases, in contrast to alteration-resistant elements such as Nb, Ta, Zr, Hf, Th, and the lanthanide rare earths. Also, although age-corrected Nd isotope ratios are not affected appreciably by the types and amounts of alteration present, the same cannot necessarily be assumed of age-corrected Pb isotope values. Moderate amounts of seawater-mediated alteration tend not to directly affect Pb isotope ratios in basalt significantly, because of the very low concentration of Pb in seawater; however, uptake of U from seawater-derived fluids and Pb (and rarely, Th) mobility within a rock during alteration can cause large changes in parent–daughter ratios [see Mahoney *et al.* (1998) and references therein]. Such alteration typically occurs within the first few million years after rock formation (e.g. Staudigel *et al.*, 1995), before Pb isotope ratios have changed significantly by radiogenic ingrowth; thus, if an altered rock behaves thereafter as a closed system to U, Th, and Pb, its age-corrected Pb isotope ratios will be close to its original, magmatic values. However, if subsequent modification of parent–daughter ratios occurs long afterward—for example, during a later alteration event(s) or even during leaching—then the age-adjusted Pb isotope ratios of old rocks will be erroneously high or low. The principal effect is on age-corrected $(^{206}Pb/^{204}Pb)_t$, followed by $(^{208}Pb/^{204}Pb)_t$; although the half-life of ^{235}U (the parent of ^{207}Pb) is much shorter than that of ^{238}U (the parent of ^{206}Pb), the effect on $(^{207}Pb/^{204}Pb)_t$ of a change in parent–daughter ratio is relatively small for Phanerozoic rocks because of the very low abundance of ^{235}U. Of course, alteration at any stage that involves fluids containing Pb derived from marine sediment or continental crust can cause significant changes to all three Pb isotope ratios.

Fortunately, several criteria can be used to evaluate the degree to which Pb isotope systematics have been disturbed (see Mahoney *et al.*, 1998): (1) for MORB- and OIB-type rocks, age-corrected Pb isotope data are suspect if they fall significantly outside the age-adjusted fields for modern MORB- and OIB-type mantle (i.e. adjusted for changes resulting from radiogenic ingrowth in the mantle); (2) age-corrected values for a group of related samples should usually have a smaller range than the present-day range; (3) acid-leached and unleached splits should yield similar age-corrected Pb isotope ratios; (4) substantial variation in $(^{206}Pb/^{204}Pb)_t$ at near-constant $\varepsilon_{Nd}(t)$ in a group of related samples (e.g. from a single

Table 1: Sr and Nd isotopic ratios and isotope-dilution concentrations

Sample		Age, t (Ma)	Nd (ppm)	Sm	Sr	Rb	$^{147}Sm/^{144}Nd$	$^{87}Rb/^{86}Sr$	$(^{143}Nd/^{144}Nd)_0$	$(^{87}Sr/^{86}Sr)_0$	$\varepsilon_{Nd}(t)$	$(^{87}Sr/^{86}Sr)_t$
Indus–Yarlung Suture												
Dajiweng		*130*										
DJB98-11			20·95	5·150	1425	4·06	0·1486	0·0083	0·512800	0·70824	+3·9	0·70823
	L		7·338	2·193	504·8	9·29	0·1807	0·0533	0·512835	0·70692	+4·1	0·70682
DJB98-18 G			3·677	1·237	611·3	1·59	0·2033	0·0075	0·513049	0·70461	+7·9	0·70460
DJB98-20			35·10	7·359	369·2	4·71	0·1268	0·0369	0·512801	0·70403	+4·3	0·70396
Bar		*130*										
BAR98-1 G			9·096	3·292	218·7	5·90	0·2188	0·0780	0·513109	0·70413	+8·8	0·70399
BAR98-3 G			5·380	1·966	448·1	69·4	0·2208	0·4481	0·513107	0·70485	+8·7	0·70402
BAR98-6			34·42	7·330	147·7	7·37	0·1287	0·1442	0·512751	0·70443	+3·3	0·70416
Dangqiong		*200*										
DQ98-9 G			8·239	3·143	191·2	0·182	0·2306	0·0028	0·513114	0·70321	+8·4	0·70320
DQ98-12 G			8·123	3·017	137·0	0·294	0·2245	0·0062	0·513114	0·70307	+8·5	0·70305
DQ98-14 D			16·91	6·068	204·6	0·400	0·2169	0·0056	0·513111	0·70295	+8·7	0·70293
Xialu		*120*										
XL98-10 D			8·011	2·705	166·3	2·11	0·2041	0·0366	0·513083	0·70345	+8·5	0·70339
Dazhuqu–Dazhuka		*120*										
DZ98-1 G			6·660	2·446	180·7	0·728	0·2220	0·0117	0·513118	0·70356	+8·9	0·70354
DZ98-12 D			7·654	2·677	128·0	0·301	0·2114	0·0068	0·513108	0·70451	+8·9	0·70450
	L		5·595	2·162	169·7	0·359	0·2355	0·0061	0·513118	0·70440	+8·7	0·70439
DZ98-19			8·642	2·896	158·1	1·82	0·2026	0·0333	0·513080	0·70433	+8·5	0·70427
Langceling		*120*										
LC98-3			4·639	1·706	98·84	3·35	0·2223	0·0980	0·513109	0·70472	+8·8	0·70455
LC98-4			3·534	1·477	130·0	10·3	0·2525	0·2291	0·513133	0·70485	+8·8	0·70446
LC98-6			2·413	1·023	82·20	5·22	0·2561	0·1836	0·513136	0·70483	+8·8	0·70451
Luobusha		*177*										
LB98-1 G			10·94	3·860	294·0	13·1	0·2134	0·1287	0·513071	0·70621	+8·0	0·70589
	L		13·46	4·707	340·3	17·0	0·2114	0·1328	0·513079	0·70610	+8·2	0·70577
LB98-3 G			5·732	2·047	118·8	0·897	0·2159	0·0218	0·513086	0·70300	+8·3	0·70295
Southern Iran												
Band-e-Zeyarat		*143*										
BZ96-4			6·826	2·286	167·6	0·627	0·2024	0·0108	0·512990	0·70377	+6·7	0·70374
	L				17·83	0·811		0·1316		0·70352		0·70325
BZ96-6 D			22·90	6·877	207·1	2·36	0·1815	0·0329	0·512948	0·70365	+6·3	0·70359
	L				18·97	1·28		0·1953		0·70358		0·70318

Sample		Age, t (Ma)	Nd (ppm)	Sm	Sr	Rb	$^{147}Sm/^{144}Nd$	$^{87}Rb/^{86}Sr$	$(^{143}Nd/^{144}Nd)_0$	$(^{87}Sr/^{86}Sr)_0$	$\varepsilon_{Nd}(t)$	$(^{87}Sr/^{86}Sr)_t$
BZ96-10			17·25	5·523	244·1	7·14	0·1936	0·0846	0·512954	0·70358	+6·2	0·70341
	L				307·0	9·59		0·0904		0·70358		0·70339
BZ97-4-1			9·547	3·251	322·4	2·65	0·2058	0·0237	0·513068	0·70440	+8·2	0·70435
	L		4·019	1·517	306·2	4·50	0·2282	0·0467	0·513088	0·70386	+8·2	0·70377
BZ97-11-5			25·63	7·437	214·9	3·71	0·1754	0·0500	0·512951	0·70349	+6·5	0·70339
BZ97-14-1			12·53	3·582	135·1	0·178	0·1728	0·0037	0·512902	0·70448	+5·5	0·70447
BZ97-14-2 D			12·15	3·449	214·1	0·126	0·1716	0·0017	0·512904	0·70444	+5·6	0·70444
BZ97-14-6			6·820	2·372	233·5	14·4	0·2102	0·1789	0·513022	0·70493	+7·2	0·70457
Neyriz		*93*										
N95-28			6·102	2·250	192·2	0·987	0·2229	0·1485	0·513060	0·70496	+7·9	0·70476
N95-33			8·136	2·844	277·9	7·71	0·2113	0·0803	0·513051	0·70379	+7·8	0·70368
N96-61			8·346	2·899	138·5	1·07	0·2100	0·0224	0·513056	0·70406	+7·9	0·70403
N96-62			6·980	2·515	134·2	0·435	0·2178	0·0094	0·513056	0·70432	+7·8	0·70431
N96-64			7·890	2·703	178·9	0·529	0·2071	0·0086	0·513046	0·70445	+7·8	0·70444
N14b G			10·62	3·665	530·4	2·32	0·2086	0·0126	0·513067	0·70671	+8·2	0·70669
Albania		*165*										
AL-1			10·62	3·813	168·7	5·82	0·2170	0·0998	0·513047	0·70387	+7·5	0·70363
	L				204·9	6·48		0·0915		0·70383		0·70361
AL-2			14·40	5·424	77·92	0·165	0·2277	0·0061	0·513041	0·70309	+7·2	0·70307
	L				80·64	0·111		0·0004		0·70298		0·70297
AL-4			9·112	3·449	69·87	0·311	0·2288	0·0129	0·513044	0·70444	+7·2	0·70441
	L				64·71	0·348		0·0156		0·70412		0·70409
IA-509			4·944	2·339	148·3	2·30	0·2860	0·0449	0·513100	0·70451	+7·1	0·70440
	L				119·8	5·78		0·1396		0·70342		0·70309
RU-124			6·001	2·764	50·03	0·137	0·2784	0·0079	0·513107	0·70365	+7·4	0·70363
	L				52·54	0·119		0·0065		0·70357		0·70356
RU-143			9·105	3·126	63·30	4·42	0·2075	0·2021	0·513052	0·70397	+7·8	0·70349
	L				84·02	2·21		0·0761		0·70372		0·70354
Seafloor off northwestern Australia												
Dredge sites		*160*										
95/10-13A			40·15	8·559	423·8	9·01	0·1292	0·0655	0·512769	0·70357	+3·9	0·70342
	L		14·08	3·627	482·5	12·8	0·1557	0·0765	0·512813	0·70354	+4·2	0·70337
95/10-15A			81·44	16·60	484·3	32·4	0·1232	0·1935	0·512747	0·70395	+3·6	0·70351
	L		20·66	5·245	587·5	31·9	0·1535	0·1569	0·512799	0·70380	+4·0	0·70344
96/23-4			47·94	11·48	389·5	9·95	0·1447	0·0739	0·512753	0·70433	+3·3	0·70416
	L		7·436	2·536	447·7	9·02	0·2061	0·0583	0·512828	0·70405	+3·5	0·70392
96/24-1			27·70	7·151	330·8	1·12	0·1560	0·0105	0·512775	0·70391	+3·5	0·70389
	L		4·893	1·384	377·3	12·8	0·1710	0·0977	0·512852	0·70385	+4·1	0·70362
		134										

Table 1: continued

Sample		Age, t (Ma)	Nd (ppm)	Sm	Sr	Rb	$^{147}Sm/^{144}Nd$	$^{87}Rb/^{86}Sr$	$(^{143}Nd/^{144}Nd)_0$	$(^{87}Sr/^{86}Sr)_0$	$\varepsilon_{Nd}(t)$	$(^{87}Sr/^{86}Sr)_t$
96/8-10A			39·21	9·181	456·0	42·5	0·1415	0·2697	0·512631	0·70756	+0·8	0·70705
	L		11·25	2·992	526·1	30·0	0·1607	0·1651	0·512653	0·70701	+0·9	0·70670
96/34-2			12·10	3·721	188·2	18·6	0·1859	0·2852	0·512930	0·70389	+5·8	0·70335
96/34-3			7·450	2·542	144·0	7·80	0·2062	0·1566	0·513003	0·70394	+6·9	0·70364
96/34-4			7·727	2·621	183·6	2·17	0·2050	0·0341	0·513001	0·70348	+6·9	0·70342
DSDP Site 261		*152*										
261-34R-2 (60–62) sill			6·687	2·691	100·4	3·03	0·2433	0·0871	0·513114	0·70307	+8·3	0·70288
261-35R-2 (87–89) sill			6·717	2·645	89·26	5·86	0·2380	0·1898	0·513126	0·70333	+8·7	0·70293
	L				75·87	2·29		0·0872		0·70319		0·70300
261-35R-4 (98–100)			21·24	7·500	120·8	13·9	0·2135	0·3328	0·513107	0·70373	+8·8	0·70301
	L		2·745	1·195	99·82	4·78	0·2632	0·1384	0·513151	0·70340	+8·7	0·70310
261-37R-2 (34–36)			4·423	1·735	101·8	12·6	0·2371	0·3566	0·513108	0·70415	+8·3	0·70338
	L				102·0	9·71		0·2754		0·70382		0·70323
ODP Site 765		*155*										
765C-63R-4 (132–134)			8·541	3·366	95·67	16·3	0·2382	0·4922	0·513124	0·70411	+8·6	0·70302
765D-21R-1 (109–111)			9·909	3·858	101·8	6·38	0·2353	0·1813	0·513107	0·70323	+8·3	0·70283
Paleotethyan sites												
Mayodia		*275*										
AP-146			8·857	2·734	106·1	0·382	0·1866	0·0104	0·513037	0·70366	+8·1	0·70362
	L				164·3	0·186		0·0033		0·70300		0·70299
AP-148			11·15	3·485	78·68	2·38	0·1890	0·0873	0·512880	0·70498	+5·0	0·70464
Lancang R. Zone (Jinghong)		*300*										
HN-4			4·528	1·890	124·6	0·772	0·2523	0·0179	0·513212	0·70593	+9·0	0·70585
Ailaoshan (Laowangzai)		*350*										
LZK 1-3			6·861	2·406	119·6	15·41	0·2120	0·3727	0·513191	0·71170	+9·8	0·70984
Changning–Menglian		*350*										
MW-10			5·899	2·122	101·9	0·212	0·2174	0·0060	0·513076	0·70368	+7·6	0·70365
MX 1+3			11·60	3·626	427·4	5·176	0·1890	0·0342	0·512894	0·70498	+5·3	0·70481

G, gabbro; D, diabase; other samples are basalt. L, strongly acid-leached powder. Isotopic fractionation corrections are $^{148}NdO/^{144}NdO = 0{\cdot}242436$ ($^{148}Nd/^{144}Nd = 0{\cdot}241572$); $^{86}Sr/^{88}Sr = 0{\cdot}1194$. Measurements were made on a VG Sector multicollector instrument at the University of Hawaii. Data are reported relative to $^{143}Nd/^{144}Nd = 0{\cdot}511850$ for the La Jolla Nd standard and $^{87}Sr/^{86}Sr = 0{\cdot}71024$ for NBS 987 Sr. Over a 3 year period bracketing the above measurements, the total range measured for NBS 987 Sr was $\pm 0{\cdot}000021$; for La Jolla Nd it was $\pm 0{\cdot}000010$ (0·2 ε units). Within-run errors on the isotopic data above are less than or equal to the external uncertainties on these standards. Total blanks are <35 pg for Sr and <10 pg for Nd. Uncertainties on Nd and Sm concentrations are estimated at $<0{\cdot}2\%$, on Sr $<0{\cdot}5\%$, and on Rb 1%. $\varepsilon_{Nd}(t) = 0$ today corresponds to $^{143}Nd/^{144}Nd = 0{\cdot}512640$; $\varepsilon_{Nd}(t) = 0$ for past times is calculated assuming $^{147}Sm/^{144}Nd = 0{\cdot}1967$. Ages are from references cited in the text. Changning–Menglian sample MW-10 is from Wumulong and MX 1+3 is from Manxin. DSDP and ODP site numbers are indicated at the beginning of a sample's name [e.g. 216-35R-2 (87–89) is Site 261, Core 35R, Section 2, Interval 87–89 cm]. Subscript 0 indicates measured isotopic composition.

Table 2: Pb isotope ratios and isotope-dilution concentrations

Sample		Age, t (Ma)	Pb (ppm)	U	Th	$^{238}U/^{204}Pb$	$^{232}Th/^{204}Pb$	Th/U	$(^{206}Pb/^{204}Pb)_0$	$(^{207}Pb/^{204}Pb)_0$	$(^{208}Pb/^{204}Pb)_0$	$(^{206}Pb/^{204}Pb)_t$	$(^{207}Pb/^{204}Pb)_t$	$(^{208}Pb/^{204}Pb)_t$
Indus–Yarlung Suture														
Dajiweng		*130*												
DJB98-11			1·563	0·4258	0·9301	17·6	39·8	2·18	19·164	15·602	39·152	18·81	15·58	38·90
	L		1·324	0·2893	0·7924	14·1	39·9	2·74	19·071	15·593	38·967	18·78	15·58	38·71
DJB98-18 G			0·1069	0·0429	0·1976	25·2	121	4·65	18·433	15·524	38·417	17·92	15·50	37·64
DJB98-20			1·163	0·6940	2·227	39·0	129	3·21	19·389	15·584	39·715	18·59	15·54	38·88
Bar		*130*												
BAR98-1 G			0·1317	0·0117	0·0303	5·56	14·9	2·59	17·970	15·479	37·948	17·86	15·47	37·85
BAR98-6			3·280	0·7946	3·936	15·8	80·7	4·95	19·132	15·629	39·524	18·81	15·61	39·00
Dangqiong		*200*												
DQ98-9 G			0·2413	0·0173	0·0304	4·42	8·05	1·76	17·627	15·420	37·458	17·49	15·41	37·38
DQ98-12 G			0·1074	0·0062	0·0093	3·55	5·57	1·52	17·707	15·434	37·500	17·60	15·43	37·45
DQ98-14 D			0·4296	0·0717	0·1296	10·4	19·3	1·81	17·759	15·414	37·526	17·43	15·40	37·33
Xialu		*120*												
XL98-10 D			0·2350	0·0488	0·0947	12·9	25·8	1·94	17·721	15·435	37·438	17·48	15·42	37·28
Dazhuqu–Dazhuka		*120*												
DZ98-1 G			0·5924	0·0160	0·0492	1·66	5·27	3·07	17·438	15·395	37·253	17·41	15·39	37·22
DZ98-12 D			0·3986	0·0392	0·0798	6·06	12·7	2·04	17·563	15·404	37·326	17·45	15·40	37·25
	L		0·3539	0·0404	0·0759	7·03	13·6	1·88	17·560	15·399	37·295	17·43	15·39	37·21
DZ98-19			0·3676	0·0336	0·0803	5·64	13·9	2·39	17·581	15·401	37·339	17·48	15·40	37·26
Langceling		*120*												
LC98-3			0·3086	0·1204	0·0504	24·3	10·5	0·42	18·128	15·465	37·550	17·67	15·44	37·49
LC98-4			0·5855	0·2319	0·0558	24·7	6·14	0·24	18·129	15·465	37·496	17·66	15·44	37·46
LC98-6			0·2784	0·0154	0·0239	3·42	5·50	1·55	17·769	15·456	37·582	17·71	15·45	37·55
Luobusha		*177*												
LB98-1 G			0·5073	0·0441	0·0444	5·42	5·64	1·01	17·972	15·478	37·731	17·82	15·47	37·68
	L		0·6137	0·0510	0·0841	5·17	8·81	1·65	17·904	15·442	37·598	17·76	15·44	37·52
LB98-3 G			0·3781	0·0131	0·0397	2·14	6·71	3·04	17·724	15·440	37·538	17·66	15·44	37·48
Southern Iran														
Band-e-Zeyarat		*143*												
BZ96-4			0·5227	0·0574	0·2223	6·92	27·7	3·88	18·212	15·523	38·260	18·06	15·52	38·06
BZ96-6 D			2·002	0·1221	0·5148	3·83	16·7	4·22	18·096	15·490	38·080	18·01	15·49	37·96
BZ96-10			0·9802	0·1075	0·5083	6·91	33·8	4·73	18·189	15·509	38·253	18·03	15·50	38·01

Table 2: continued

Sample		Age, t (Ma)	Pb (ppm)	U	Th	$^{238}U/^{204}Pb$	$^{232}Th/^{204}Pb$	Th/U	$(^{206}Pb/^{204}Pb)_0$	$(^{207}Pb/^{204}Pb)_0$	$(^{208}Pb/^{204}Pb)_0$	$(^{206}Pb/^{204}Pb)_t$	$(^{207}Pb/^{204}Pb)_t$	$(^{208}Pb/^{204}Pb)_t$
BZ97-4-1			1·073	0·0641	0·0638	3·70	3·79	1·00	17·697	15·404	37·459	17·61	15·40	37·43
	L		0·9223	0·0518	0·0614	3·47	4·26	1·19	17·702	15·405	37·457	17·62	15·40	37·43
BZ97-11-5			2·300	0·2417	0·8237	6·61	23·3	3·41	18·129	15·498	38·127	17·98	15·49	37·96
BZ97-14-1			0·9133	0·2720	0·6934	18·9	49·9	2·55	18·511	15·537	38·421	18·09	15·52	38·07
BZ97-14-2 D			1·981	0·2925	0·6934	9·33	22·8	2·37	18·316	15·528	38·257	18·11	15·52	38·10
BZ97-14-6			0·4535	0·0987	0·2942	13·8	42·5	2·98	18·399	15·533	38·381	18·09	15·52	38·08
Neyriz		*93*												
N95-28			0·4040	0·0471	0·0965	7·30	15·4	2·05	18·047	15·473	37·903	17·94	15·47	37·83
N95-33			0·1560	0·0508	0·1308	20·5	54·5	2·58	18·275	15·464	38·030	17·98	15·45	37·78
N96-61			0·4373	0·0747	0·1813	10·7	26·9	2·43	18·168	15·473	37·955	18·01	15·47	37·83
N96-62			0·3697	0·0639	0·1414	10·8	24·8	2·21	18·152	15·477	37·954	18·00	15·47	37·84
N96-64			0·2389	0·0659	0·1488	17·3	40·4	2·26	18·227	15·474	38·011	17·98	15·46	37·82
N14B G			0·3267	0·0879	0·2321	16·9	46·0	2·64	18·149	15·444	37·999	17·90	15·43	37·79
Albania		*165*												
AL-1			0·5491	0·0170	0·0454	1·94	5·35	2·67	18·145	15·474	37·795	18·10	15·47	37·75
AL-2			0·3164	0·0255	0·0920	5·11	19·0	3·61	15·520	15·501	38·287	18·39	15·49	38·13
	L		0·2223	0·0215	0·0626	6·08	18·3	2·91	18·304	15·488	38·009	18·15	15·48	37·86
AL-4			0·1091	0·0565	0·1225	33·0	73·9	2·17	18·620	15·531	38·558	17·76	15·49	37·95
IA-509			0·1036	0·0214	0·0587	13·2	37·4	2·74	18·856	15·491	38·632	18·51	15·47	38·32
RU-124			0·4869	0·0209	0·0770	2·68	10·2	3·69	18·103	15·470	37·755	18·03	15·47	37·67
RU-143			0·0845	0·0404	0·1822	30·7	143	4·51	18·910	15·529	38·953	18·11	15·49	37·78
Seafloor off northwestern Australia														
Dredge sites		*160*												
95/10-13A			1·983	0·4627	1·661	15·1	56·1	3·59	19·185	15·567	39·236	18·80	15·55	38·79
	L		2·293	0·1413	0·2544	3·96	7·37	1·80	18·925	15·552	38·863	18·83	15·55	38·80
95/10-15A			5·797	1·243	5·112	14·0	59·4	4·11	19·379	15·592	39·479	19·03	15·58	39·01
	L		2·240	0·3936	0·9430	11·4	28·1	2·40	19·219	15·559	38·992	18·93	15·54	38·77
96/23-4			2·400	0·4771	2·634	12·9	73·4	5·52	19·120	15·619	39·104	18·80	15·60	38·52
	L		0·8582	0·1150	0·2638	8·62	20·4	2·29	18·988	15·593	38·878	18·77	15·58	38·72
96/24-1			1·390	0·2542	1·074	11·8	51·6	4·23	19·163	15·609	38·995	18·87	15·59	38·58
	L		0·5053	0·0835	0·2092	10·6	27·4	2·51	18·918	15·593	38·692	18·65	15·58	38·47
		134												

JOURNAL OF PETROLOGY | VOLUME 46 | NUMBER 4 | APRIL 2005

Sample		Age, t (Ma)	Pb (ppm)	U	Th	$^{238}U/^{204}Pb$	$^{232}Th/^{204}Pb$	Th/U	$(^{206}Pb/^{204}Pb)_0$	$(^{207}Pb/^{204}Pb)_0$	$(^{208}Pb/^{204}Pb)_0$	$(^{206}Pb/^{204}Pb)_t$	$(^{207}Pb/^{204}Pb)_t$	$(^{208}Pb/^{204}Pb)_t$
96/8-10A			9·043	1·318	7·057	9·43	52·2	5·35	18·746	15·714	39·397	18·55	15·70	39·05
	L		6·352	0·8176	3·088	8·31	32·4	3·78	18·722	15·701	39·293	18·55	15·69	39·08
96/34-2			0·9777	0·1942	0·6091	12·5	40·6	3·14	18·270	15·530	38·201	18·01	15·52	37·93
96/34-3			0·4613	0·1049	0·2797	14·3	39·5	2·67	18·294	15·527	38·112	17·99	15·51	37·85
96/34-4			0·5488	0·1069	0·2427	12·2	28·7	2·27	18·092	15·523	38·029	17·84	15·51	37·84
DSDP Site 261		*152*												
261-34R-2 (60–62) sill			0·1198	0·1143	0·0457	60·2	24·9	0·40	18·871	15·525	37·618	17·44	15·45	37·43
261-35R-2 (87–89) sill			0·2998	0·2874	0·0518	60·3	11·2	0·18	18·781	15·515	37·494	17·34	15·44	37·41
	L		0·1513	0·157	0·0089	65·4	3·85	0·06	18·900	15·524	37·483	17·34	15·45	37·45
261-35R-4 (98–100)			0·6038	1·011	0·4523	108	50·1	0·45	20·184	15·609	38·078	17·60	15·48	37·70
	L		0·2190	0·1570	0·3274	47·1	101	2·09	21·011	15·671	38·289	19·89	15·62	37·52
261-37R-2 (34–36)			0·1927	0·0393	0·0561	12·7	18·8	1·43	18·160	15·497	37·664	17·86	15·48	37·52
	L		0·0758	0·0181	0·0118	15·0	10·0	0·65	18·191	15·489	37·646	17·83	15·47	37·57
ODP Site 765		*155*												
765C-63R-4 (132–134)			0·3140	0·5413	0·0621	110	13·0	0·12	19·728	15·552	37·483	17·05	15·42	37·38
765D-21R-1 (109–111)			0·3425	0·0716	0·1268	13·1	23·9	1·77	18·125	15·475	37·734	17·81	15·46	37·55
Paleotethyan sites														
Mayodia		*275*												
AP-146			1·216	0·3671	1·208	19·0	64·6	3·29	18·256	15·485	38·030	17·43	15·44	37·15
AP-148			1·089	0·1762	0·8593	10·1	51·0	4·88	17·969	15·460	37·943	17·53	15·44	37·24
Lancang R. (Jinghong)		*300*												
HN-4			0·5930	0·0274	0·0255	2·94	2·82	0·93	18·408	15·604	38·386	18·27	15·60	38·34
Ailaoshan (Laowangzai)		*350*												
LZK 1-3			1·551	0·0623	0·0525	2·56	2·23	0·84	18·483	15·682	38·661	18·34	15·67	38·62
Changning–Menglian		*350*												
MW-10			0·4615	0·0430	0·1038	5·78	14·4	2·41	17·620	15·437	37·649	17·30	15·42	37·40
MX 1+3			0·5000	0·1218	0·4234	15·7	56·2	3·48	18·622	15·542	39·217	17·75	15·50	38·24

Pb isotope ratios are corrected for fractionation using the NBS 981 standard values of Todt *et al.* (1996). The total ranges measured for NBS 981 in a 3 year period bracketing the analyses are ±0·011 for $^{206}Pb/^{204}Pb$, ±0·010 for $^{207}Pb/^{204}Pb$, and ±0·032 for $^{208}Pb/^{204}Pb$. Within-run errors on the isotopic data above are less than or equal to these values. Estimated uncertainty on Pb concentrations is 0·5%, on U ~1%, and on Th ~2%. Propagation of errors on age-corrected Pb isotope ratios: for a 150 Ma sample with $^{238}U/^{204}Pb = 30$ and $^{232}Th/^{204}Pb = 100$, a maximum error on parent–daughter ratios translates to an additional error of ±0·011 on $(^{206}Pb/^{204}Pb)_t$, ±0·005 on $(^{207}Pb/^{204}Pb)_t$, and ±0·019 on $(^{208}Pb/^{204}Pb)_t$. Total procedural blanks are 5–35 pg for Pb, <5 pg for U, and <3 pg for Th. Subscript 0 indicates measured isotopic composition.

Table 3: Bulk-rock incompatible trace-element concentrations (ppm)

Sample	Rb	Sr	Y	Zr	Nb	Ba	La	Ce	Pr	Nd	Sm	Eu	Tb	Gd	Dy	Ho	Er	Tm	Yb	Lu	Hf	Ta	Pb	Th	U
Indus–Yarlung suture zone, Tibet																									
DJB98-19 G	0·43	183	21·7	46	1·3	32	1·64	5·52	0·877	4·91	1·93	0·70	0·45	2·63	3·63	0·81	2·38	0·35	2·25	0·34	1·37	0·09	0·11	0·14	0·06
DJB98-12	6·8	754	24·3	145	16	181	11·3	26·4	3·79	17·2	4·52	1·56	0·74	4·67	4·85	0·91	2·49	0·33	2·05	0·28	3·60	1·11	1·15	1·53	0·39
DJB98-20	5·3		24·1	261	41	108	22·7	44·2	6·68	28·1	6·54	2·08	0·94	6·44	5·18	0·94	2·34	0·31	1·89	0·26	5·51	2·56	0·99	1·69	0·86
DJB98-18 G	3·9		13·6	29	0·52	80	1·61	4·39	0·746	3·93	1·25	0·53	0·31	1·78	2·02	0·52	1·55	0·24	1·47	0·22	0·89	0·04	0·16	0·19	0·05
DJB98-11	3·5		26·0	171	20	133	13·9	28·5	4·43	19·5	5·11	1·74	0·82	5·21	4·70	0·97	2·61	0·35	2·16	0·31	4·00	1·31	1·50	1·67	0·48
BAR98-1 G	6·7	158	28·4	95	1·3	159	2·73	7·67	1·59	8·28	2·76	1·06	0·69	3·84	4·51	1·06	2·94	0·45	2·86	0·43	2·45	0·10	0·26	0·08	0·04
BAR98-3 G	45	355	17·3	38	0·61	389	1·51	4·99	0·911	4·56	1·68	0·78	0·41	2·30	2·90	0·64	1·75	0·27	1·75	0·26	1·35	0·05	0·63	0·05	0·02
BAR98-6	7·6	137	23·1	233	42	94	27·9	60·8	7·75	30·7	6·66	2·06	0·93	6·28	4·73	0·90	2·26	0·29	1·82	0·24	4·94	2·37	3·30	4·05	0·90
DQ98-14 D	0·51		63·7	188	3·2	9·4	5·35	18·3	3·34	18·5	6·58	1·85	1·49	8·37	9·87	2·41	6·96	1·01	6·30	0·92	4·74	0·21	0·61	0·18	0·08
DQ98-16 G	0·14	122	20·5	28	0·89	4·0	1·18	4·00	0·830	5·02	2·05	0·87	0·52	2·84	3·55	0·82	2·30	0·32	2·16	0·31	0·77	0·07	0·14	0·02	0·01
DQ98-12 G	0·19	111	24·5	56	1·0	3·2	1·46	6·22	1·06	6·05	2·30	0·85	0·60	3·06	3·85	0·90	2·57	0·38	2·44	0·37	1·63	0·08	0·14	0·01	0·01
DQ98-9 G	0·21	162	30·1	90	1·2	6·6	2·11	6·82	1·36	7·68	2·89	0·95	0·72	3·93	4·95	1·13	3·39	0·47	3·15	0·48	2·45	0·10	0·23	0·04	0·04
DQ98-18 D	0·19	58	28·0	52	1·6	2·3	1·49	5·74	1·16	7·26	2·88	1·08	0·73	3·95	4·77	1·13	3·13	0·45	2·83	0·42	1·18	0·10	0·14	0·03	0·01
XL98-10 D	1·6	185	24·8	87	1·9	5·9	3·10	8·08	1·65	8·15	2·69	1·00	0·64	3·55	4·24	0·94	2·58	0·39	2·48	0·37	2·01	0·14	0·18	0·13	0·05
XL98-15 D	1·5	97	24·9	80	0·95	3·2	2·22	7·29	1·36	7·06	2·51	0·90	0·59	3·33	4·28	0·94	2·62	0·40	2·55	0·37	1·99	0·07	0·13	0·08	0·03
YZS-1	12		22·6	68	1·2	11	2·17	7·51	1·29	6·84	2·49	0·97		3·50	4·49				2·62	0·39	1·95	0·09	0·25	0·10	0·07
YZS-3	18		24·1	64	1·2	12	2·37	7·75	1·36	7·04	2·48	1·08		3·55	4·70				2·79	0·40	1·92	0·09	0·45	0·09	0·07
YZS-6	5·6		28·2	88	1·5	8·9	3·13	10·2	1·79	9·30	3·41	1·25		4·43	5·67				3·39	0·44	2·57	0·10	0·52	0·11	0·07
YZS-11	8·6		26·6	83	1·3	8·1	2·92	9·56	1·71	8·60	3·01	1·18		3·82	5·10				2·80	0·41	2·35	0·09	0·49	0·10	0·05

Sample	Rb	Sr	Y	Zr	Nb	Ba	La	Ce	Pr	Nd	Sm	Eu	Tb	Gd	Dy	Ho	Er	Tm	Yb	Lu	Hf	Ta	Pb	Th	U
DZ98-1 G	0·90		24·7	64	0·74	3·9	1·83	6·30	1·14	6·54	2·44	0·86	0·58	3·18	3·85	0·94	2·80	0·40	2·47	0·38	1·78	0·07	0·66	0·05	0·02
DZ98-12 D	0·40		24·3	84	0·77	3·7	1·81	6·61	1·07	5·86	2·19	0·73	0·52	2·86	3·45	0·87	2·50	0·39	2·49	0·38	2·21	0·07	0·46	0·08	0·04
DZ98-14 D	4·2	212	19·7	69	1·0	8·6	2·10	6·58	1·24	6·53	2·44	0·88	0·52	3·00	3·44	0·77	2·28	0·31	2·02	0·31	1·71	0·09	0·10	0·07	0·04
DZ98-21	10	97	18·7	57	0·67	25	2·00	4·90	1·07	5·84	2·15	0·72	0·48	2·72	3·18	0·71	2·09	0·30	1·90	0·30	1·51	0·07	0·34	0·06	0·15
DZ98-18 G	0·39		19·8	65	0·81	10	1·92	2·32	1·01	5·34	1·91	0·72	0·46	2·58	3·18	0·70	1·98	0·29	1·81	0·28	1·61	0·08	0·45	0·06	0·03
DZ98-4 D	0·36	188	22·6	75	1·2	4·5	2·49	7·82	1·41	7·17	2·49	0·93	0·56	3·25	3·89	0·86	2·38	0·36	2·31	0·34	1·85	0·09	0·11	0·10	0·04
DZ98-19	1·5	134	23·7	88	1·3	6·4	2·98	9·44	1·61	8·10	2·64	1·00	0·60	3·39	4·13	0·91	2·48	0·38	2·34	0·34	2·03	0·10	0·57	0·10	0·04
LC98-4	4·3	95	14·9	36	0.·32	7·4	0·91	2·71	0·534	3·04	1·25	0·54	0·34	1·85	2·48	0·55	1·54	0·24	1·56	0·23	1·04	0·03	0·51	0·04	0·23
LC98-3	3·9	109	20·5	56	0·83	12	1·52	5·20	1·00	5·21	1·99	0·78	0·48	2·71	3·60	0·79	2·24	0·34	2·18	0·33	1·58	0·07	0·38	0·07	0·16
LC98-6	6·3	79	11·5	25	0·30	19	0·64	2·08	0·401	2·44	1·02	0·45	0·27	1·42	2·05	0·45	1·31	0·19	1·32	0·21	0·81	0·04	0·64	0·03	0·03
LB98-1 G	18		37·0	109	1·9	55	2·89	10·0	1·79	10·1	3·72	1·33	0·85	4·79	5·80	1·43	4·22	0·60	3·73	0·57	3·03	0·16	0·66	0·08	0·04
LB98-3 G	1·6	134	18·9	58	0·98	7·1	1·91	6·15	1·08	5·79	2·08	0·79	0·48	2·69	3·07	0·74	2·10	0·29	1·87	0·29	1·58	0·09	0·40	0·09	0·03
Neyriz, Iran																									
N95-28	1·0	150	18·9	48	1·1	40	1·61	5·05	0·858	4·65	1·62	0·63	0·43	2·30	2·92	0·70	1·97	0·31	1·99	0·29	1·30	0·08	0·36	0·09	0·05
N96-62	0·68	159	24·2	68	1·5	30	2·23	6·87	1·13	6·04	2·11	0·82	0·56	2·96	3·74	0·88	2·55	0·40	2·51	0·40	1·85	0·11	0·63	0·17	0·07
N14b G	3·5		35·8	112	2·5	59	4·11	12·2	2·13	10·7	3·69	1·36	0·87	4·93	6·00	1·34	3·75	0·58	3·60	0·55	2·70	0·16	0·45	0·25	0·09
BHVO meas.	9·6	388	25·6	180	19·4	133	15·5	37·7	5·50	24·5	6·20	2·05	0·95	6·27	5·38	1·00	2·58	0·33	2·00	0·272	4·33	1·18	2·14	1·20	0·40
BHVO pref.	9·5	390	25·8	180	19·5	133	15·5	38·0	5·45	24·7	6·17	2·06	0·95	6·22	5·25	1·00	2·56	0·33	1·98	0·278	4·30	1·20	2·10	1·26	0·42

D, diabase; G, gabbro; other samples are basalt. The YZS samples are from the pillow-lava section in the Xialu area [isotopic data for these samples have been given by Mahoney *et al.* (1998)]. The relative precision for most elements is 3% or better at the 0·2–1 ppm abundance level in the rock (range is 1–8%, except for Nb, for which it is 11%). An indication of accuracy (trueness) is given by measured (mean of 15 runs) and preferred values (Eggins *et al.*, 1997; Y value is from Govindaraju, 1989) for the BHVO-1 standard. Measurements were made on a VG PQ II-S instrument at the University of Hawaii following Jain & Neal (1996).

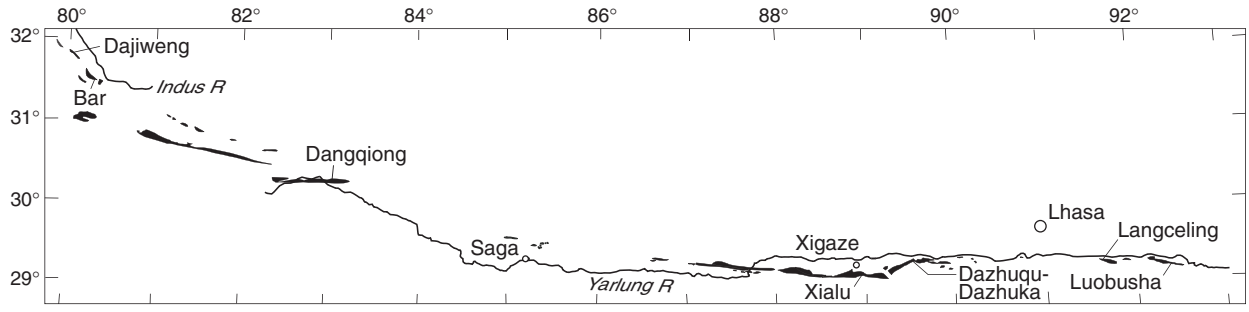

Fig. 2. Location of main ophiolite bodies (black) along the Indus and Yarlung river drainages in Tibet.

ophiolite or drill site) is a sign of disturbance of the U–Pb system; (5) data for related samples that exhibit a large dispersion of present-day $^{208}Pb/^{204}Pb$ vs $^{232}Th/^{204}Pb$ and $^{206}Pb/^{204}Pb$ vs $^{238}U/^{204}Pb$ should roughly parallel reference isochrons of the correct age.

RESULTS

Indus–Yarlung suture zone, Tibet

We collected Early Jurassic to Early Cretaceous Neotethyan magmatic rocks in 1998 from outcrops along ~1300 km of the Indus–Yarlung suture zone (Fig. 2). Radiolarians in cherts in depositional contact with pillow lavas indicate an age of ~120–125 Ma for crust of the Xigaze massif around Xialu and Dazhuqu–Dazhuka (Ziabrev *et al.*, 2003). For both sections, we sampled both the upper (pillow lavas) and lower (sills or gabbros) crustal levels. Basalts near Langceling may be an eastward extension of the same terrane, termed the Dazhuqu terrane by Aitchison *et al.* (2000). For gabbroic bodies at Luobusha, a 177 Ma Sm–Nd age has been determined (Zhou *et al.*, 2002). The Dangqiong samples are from sheeted dikes in the northern Zhongba ophiolite. Chert in this ophiolite contains latest Triassic to earliest Jurassic radiolarians and calcareous microfossils (Y.-J. Wang, unpublished data, 2001); accordingly, we use an age of 200 Ma. Basalts and gabbros in the Bar area are in an ophiolitic mélange and lack good age control, but to the west of Bar a Late Jurassic to Early Cretaceous age has been determined for radiolarian chert atop pillow basalt at Dajiweng (X.-X. Mo *et al.*, unpublished data, 2002); an age of 130 Ma is used here for samples from both areas. For most of the Tibetan samples, age-corrected $\varepsilon_{Nd}(t)$ values and Pb and Sr isotope ratios are not very sensitive to the exact age used because Sm/Nd ratios are not too far removed from the chondritic value and U/Pb, Th/Pb, and Rb/Sr ratios are generally low.

Incompatible elements

Alteration effects are most evident in highly variable concentrations of Rb, Ba, and U relative to elements such as Nb, La, and Th (Fig. 3). Small peaks or troughs at Pb are also likely to be a result of Pb mobility during alteration (see Mahoney *et al.*, 1998). Three Langceling patterns stand out in having particularly large peaks at U, and two of these also have prominent Pb peaks (Fig. 3d); it is not clear whether these peaks are solely an alteration feature or not, as these basalts are not visibly more altered than some from other locations.

Four basalts from Dajiweng and one from Bar display OIB- or enriched- (E-) MORB-like patterns, with pronounced light rare earth element enrichment and $(Nb/La)_n$ and $(Ta/La)_n > 1$ (where the subscript n indicates normalization to primitive mantle). Dajiweng gabbro DJB98-19 exhibits a flatter pattern similar to those of transitional (T-) MORB. However, most of our samples resemble normal (N-) MORB in their alteration-resistant elements. For example, $(La/Sm)_n = 0{\cdot}3–0{\cdot}8$, $(Nb/La)_n = 0{\cdot}4–1{\cdot}0$, and $(Th/Nb)_n = 0{\cdot}2–0{\cdot}8$ in all of the Dangqiong dikes, the Xialu and Dazhuqu–Dazhuka basalts and gabbros, two of the Langceling basalts, and the Luobusha and Bar gabbros. In many of these rocks, particularly the gabbros, the more incompatible alteration-resistant elements, although within the range for N-MORB globally, tend to be lower than the N-MORB average (see average N-MORB and 'D-MORB' patterns in Fig. 3a).

The Dazhuqu terrane, which includes the Xigaze massif, is structurally and petrologically the best studied area we sampled. It has been suggested to represent lithosphere formed at a mid-ocean ridge (e.g. Pozzi *et al.*, 1984; Girardeau *et al.*, 1985; Pearce & Deng, 1988), an intra-oceanic fore-arc (Aitchison *et al.*, 2000; Zhang & Zhou, 2001), or an intra-oceanic back-arc spreading center (e.g. Zhang & Zhou, 2001; Griselin, 2001). The characteristics of alteration-resistant incompatible elements in our crustal samples from Xialu and Dazhuqu–Dazhuka are consistent with an ocean-ridge origin; however, they are also compatible with a back-arc origin and do not rule out a fore-arc setting for the terrane as a whole.

The next best studied ophiolite in Tibet is the Luobusha ophiolite, which consists largely of peridotite

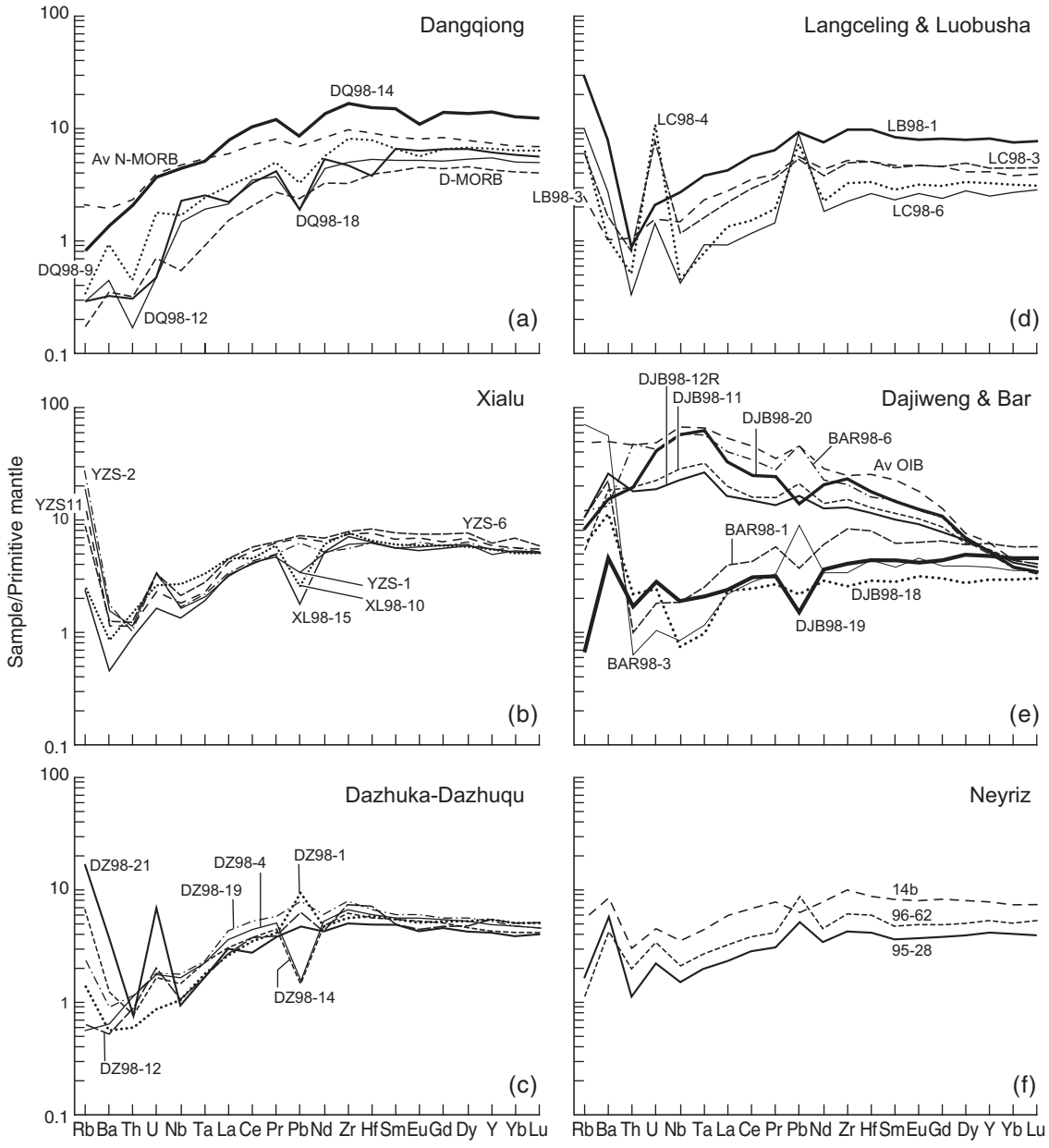

Fig. 3. Primitive-mantle-normalized incompatible element patterns of samples from the Indus–Yarlung suture zone (a–e) and Neyriz (f). Shown for comparison are patterns for worldwide average N-MORB (a) and average OIB (e) from Sun & McDonough (1989). D- ('depleted') MORB average pattern in (a) is from data of Niu & Batiza (1997). Primitive mantle normalizing values are those estimated by Sun & McDonough (1989).

interpreted to be residual MORB-type mantle, through portions of which a boninitic melt percolated after a plate-boundary reorganization placed it above a subduction zone (Zhou *et al.*, 1996). Our Luobusha samples are from gabbro bodies within the peridotite. Their essentially N-MORB-like element patterns in Fig. 3 [and basaltic major element composition (Mo *et al.*, 2005); see Electronic Appendix] suggest they represent magmas derived from the original MORB-source mantle rather than later boninitic melts.

Element patterns diagnostic of subduction-zone settings are rare in the sections we sampled. Among the alteration-resistant elements, a pronounced depletion of Nb and Ta relative to Th is typical of arc-related volcanic rocks and common in back-arc environments (e.g. Sinton *et al.*, 2003), but rare in MORB. Only one sample, Dajiweng gabbro DJB98-18, shows a significant trough at Nb–Ta relative to Th, with $(Th/Nb)_n = 3{\cdot}0$ (Fig. 3e). Because of limited exposure, this rock's field relationship with the nearby OIB-like pillow basalts and

T-MORB-like gabbro is unclear. Our only other sample with $(Th/Nb)_n > 1$ is Langceling basalt LC98-4, with a value of 1·1. In contrast, two Dazhuqu-terrane gabbros and two basalts with $(Th/Nb)_n$ significantly greater than unity (1·5–2·0) were reported by Xu & Castillo (2004); their samples also possess markedly higher Pb concentrations (0·9–2 ppm) than any of our broadly N-MORB-like Tibetan rocks (0·1–0·66 ppm). Argued to be most consistent with a back-arc affinity, their samples are from an outcrop to the west of Xialu and one SE of Dazhuka. Adjacent to the Dazhuqu terrane, true arc-type rocks are known to be prevalent in the Zedong terrane (Aitchison *et al.*, 2000; McDermid *et al.*, 2002), which, however, we did not sample.

Isotope ratios

Age-corrected $\varepsilon_{Nd}(t)$ values of the samples with broadly MORB-like incompatible element patterns cover only a small range between +8·2 and +8·9. (Unless stated otherwise we refer to values for leached splits when both leached and unleached splits were analyzed.) Despite variable alteration, their age-corrected Pb isotope ratios also fall within a small range; for samples from a single area the maximum variation in $(^{206}Pb/^{204}Pb)_t$ is only 0·15, and the total range for the MORB-like rocks as a group is only 0·45 (17·41–17·86). Minor differences are apparent from one location to another, but the small overall Nd and Pb isotopic range is remarkable, considering that the samples represent widely separated sections along 1190 km of the suture zone (i.e. from Bar to Luobusha; Fig. 2) and span ~80 Myr of time. Previous data for six pillow lavas from Xialu (Mahoney *et al.*, 1998) are in the same range as our results; so too are Göpel *et al.*'s (1984) $(^{207}Pb/^{204}Pb)_t$–$(^{206}Pb/^{204}Pb)_t$ data for several Xigaze-massif basalts. Importantly, all samples of this group display a strongly Indian-MORB-like character in Fig. 4 (for clarity, the figure is divided into panels according to sample age).

Indian-Ocean-type isotopic characteristics are also exhibited by the OIB-like Dajiweng and Bar rocks and the high-$(Th/Nb)_n$ Dajiweng gabbro from the two westernmost areas sampled. Data for the OIB-like rocks fall close to the age-adjusted field of source mantle for the modern Indian Ocean hotspot islands of Réunion, Mauritius, Crozet, and Amsterdam (Re–Cr–Am in Fig. 4). The high-$(Th/Nb)_n$ sample has slightly higher $(^{206}Pb/^{204}Pb)_t$ (17·92) and slightly lower $\varepsilon_{Nd}(t)$ (+7·9) than the broadly MORB-like samples from more easterly sections. Xu & Castillo's (2004) high-$(Th/Nb)_n$ samples also have Nd–Pb and Pb–Pb isotope ratios close to or overlapping with those of our MORB-like rocks. In short, all of the Nd–Pb and Pb–Pb isotope data for samples from ~1300 km of the Indus–Yarlung suture zone indicate a consistently Indian-Ocean-type character.

In Nd–Sr isotope space (Fig. 5), the data extend from within the MORB or Re–Cr–Am fields to higher $(^{87}Sr/^{86}Sr)_t$. This variation is attributable to the variable but pervasive seawater-mediated alteration in these rocks, in which plagioclase (the main carrier of Sr) is invariably albitized, and olivine and once-glassy groundmass are replaced by secondary phases (e.g. Girardeau *et al.*, 1985; Mo *et al.*, 2005). We subjected three of the visibly most altered samples to multi-step leaching. Differences in $\varepsilon_{Nd}(t)$ (≤0·2) and $(^{206}Pb/^{204}Pb)_t$ (0·02–0·06) between unleached and leached splits are negligible. Leaching reduced $(^{87}Sr/^{86}Sr)_t$ modestly for two samples, but by a large amount (0·70682 vs 0·70823) for OIB-like pillow lava DJB98-11. Such large decreases are commonly observed when alteration has not affected the main Sr-bearing phase(s) in a rock uniformly; in some cases, near-magmatic Sr isotope ratios have been recovered by leaching [e.g. Mahoney *et al.* (1998) and references therein]. However, in this instance the value of the leached split is still much greater than that of pillow lava DJB98-20 from the same section (0·70396). Moreover, the value of the unleached split of DJB98-11 is much higher than that of seawater itself around the time these lavas were erupted (0·7070–0·7073; e.g. Burke *et al.*, 1982); thus, DJB98-11 must contain secondary Sr from another source besides seawater. We speculate that this rock was affected by later fluids carrying continentally derived Sr, perhaps during Tertiary uplift. In any case, the effect on Nd and Pb isotopes was rather small (compare values for DJB98-11 and -20 in Tables 1 and 2).

Southern Iran

The Iranian rocks are from the Band-e-Zeyarat complex in the Makran prism, and the Neyriz ophiolite in the Zagros suture zone. Recent ^{40}Ar–^{39}Ar dating reveals an age around 143 Ma for the Band-e-Zeyarat complex (Ghazi *et al.*, 2004; see also Kananian *et al.*, 2001), whereas major and trace element data indicate a generally T-MORB-like character (Hassanipak *et al.*, 1996; Ghazi *et al.*, 2004). For Neyriz, Babaie *et al.* (2003) reported ~93 Ma ^{40}Ar–^{39}Ar ages. Mafic crustal rocks at Neyriz principally have MORB-like major and trace element compositions (Sarkarinejad, 1994), and are interpreted to represent lithosphere formed at two spreading segments offset by a transform fault (Nadimi, 2002). Few combined rare-earth and non-rare-earth trace element data are available, however, so we measured a suite of incompatible elements for three of our Neyriz basalts (Table 3). The alteration-resistant elements indeed illustrate a generally N-MORB-like character (Fig. 3f).

As with the Tibetan rocks, alteration is reflected in large $(^{87}Sr/^{86}Sr)_t$ variation accompanied by only limited variation in age-corrected Nd and Pb isotope ratios. Among the Band-e-Zeyarat samples, leached splits

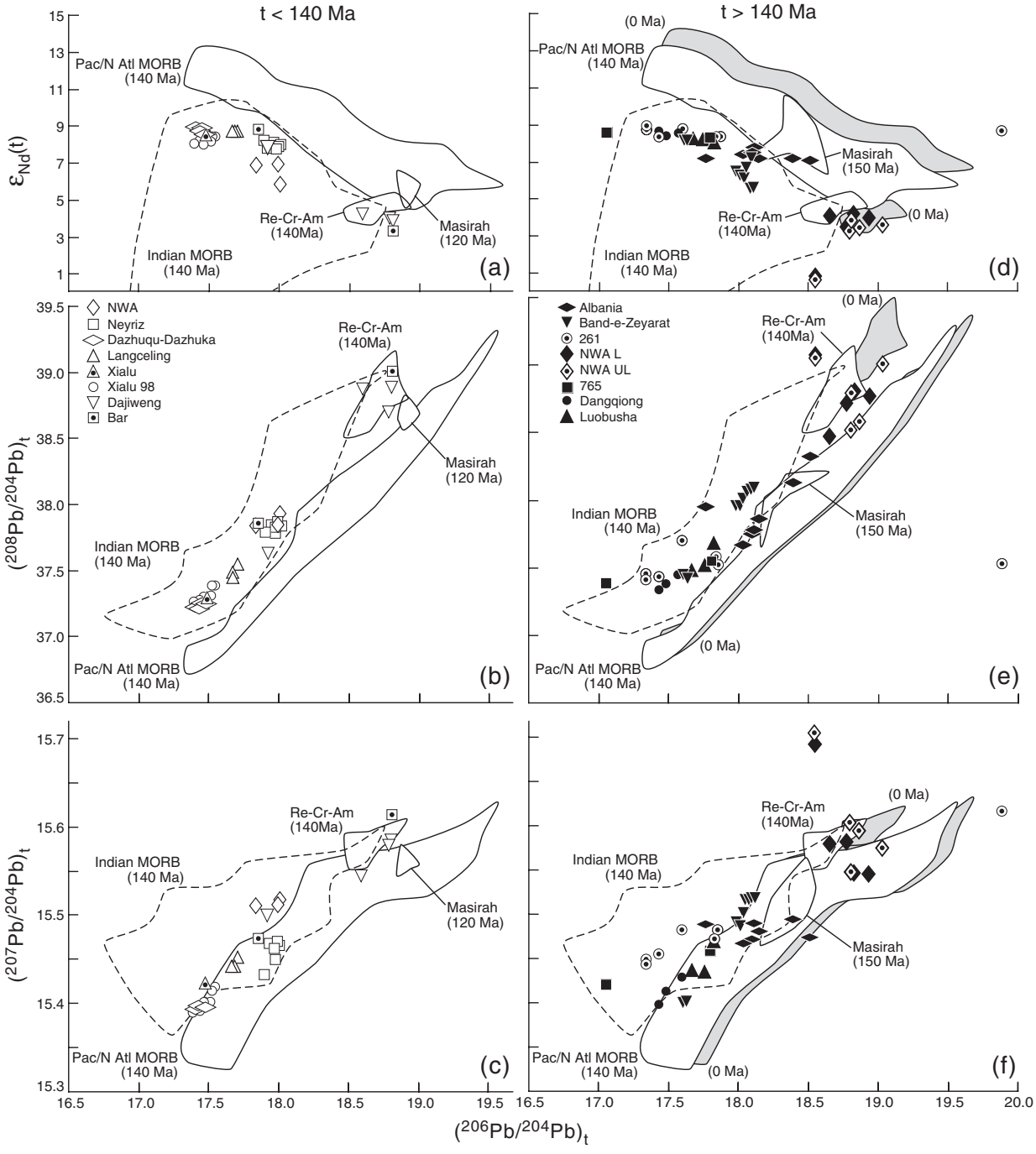

Fig. 4. Age-corrected $\varepsilon_{Nd}(t)$, $(^{208}Pb/^{204}Pb)_t$, and $(^{207}Pb/^{204}Pb)_t$ vs $(^{206}Pb/^{204}Pb)_t$ for Neotethyan samples with ages <140 Ma (a–c) and >140 Ma (d–f). For clarity, data for leached (L) and unleached (UL) samples are indicated only for the northwestern Australian dredge samples (NWA) in (d–f). Gray indicates present-day (0 Ma) fields for Pacific–North Atlantic MORB and for the Réunion and Mauritius shield volcanoes and Crozet and Amsterdam islands (Re–Cr–Am). Estimated 140 Ma fields for MORB and Re–Cr–Am mantle are unshaded and were positioned assuming $^{238}U/^{204}Pb = 5$ and 12, $^{232}Th/^{238}U = 2{\cdot}3$ and 3·3, and $^{147}Sm/^{144}Nd = 0{\cdot}24$ and 0·17 in the MORB source and Re–Cr–Am source mantle, respectively (see White, 1993; Peng & Mahoney, 1995). Data sources for the Re–Cr–Am field are those of Mahoney *et al.* (1998, 2002), plus Sheth *et al.* (2003). The fields for Pacific–North Atlantic MORB and Indian MORB are from data sources of Mahoney *et al.* (1998, 2002) and encompass >95% of the data available; the Indian MORB field includes samples between 126°E and 25·5°E. Xialu 98 data and the fields of 150 Ma N- and T-MORB and 120 Ma alkalic OIB-type basalts of Masirah are from Mahoney *et al.* (1998). Analytical errors are smaller than the size of symbols in (a) and (d); errors on $(^{208}Pb/^{204}Pb)_t$ are similar to or slightly larger than the height of the symbols; and errors on $(^{207}Pb/^{204}Pb)_t$ are less than three times the height of the smallest symbols.

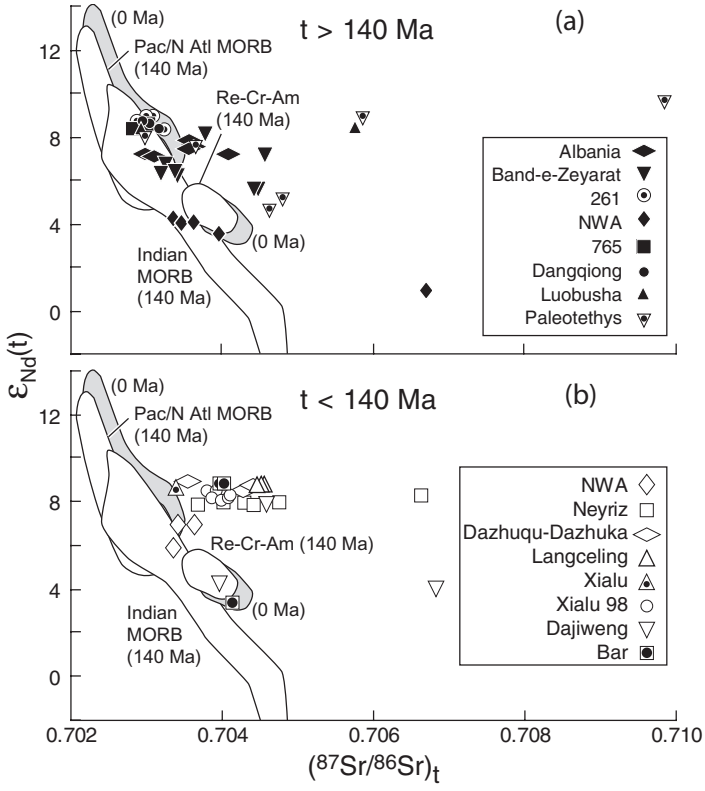

Fig. 5. Age-corrected $\varepsilon_{Nd}(t)$ vs $(^{87}Sr/^{86}Sr)_t$ for samples with ages >140 Ma (a) and <140 Ma (b). For samples with data on both unleached and leached splits, only the values for leached splits are shown. As in Fig. 4, the gray fields are for modern Pacific–North Atlantic MORB, and Réunion and Mauritius shield volcanoes and Crozet and Amsterdam islands (Re–Cr–Am). The unshaded fields are again the estimated 140 Ma positions for the MORB and island mantle sources, and additionally assume that $^{87}Rb/^{86}Sr = 0{\cdot}02$ and $0{\cdot}10$ in the MORB source and Re–Cr–Am sources, respectively (see Peng & Mahoney, 1995). Data sources used for constructing these fields are as in Fig. 4. Analytical errors are smaller than the size of symbols.

yielded systematically lower $(^{87}Sr/^{86}Sr)_t$, by as much as 0·0006, indicating partial removal of the seawater-derived Sr overprint. The $\varepsilon_{Nd}(t)$ values range from +8·2 to +5·5; however, five of the eight Band-e-Zeyarat rocks have values between +7·2 and +6·2. The sample with the highest $\varepsilon_{Nd}(t)$ has the lowest $(^{206}Pb/^{204}Pb)_t$ (17·62), and its leached and unleached splits gave essentially identical age-corrected Pb and Nd isotope ratios. For the other seven samples, $(^{206}Pb/^{204}Pb)_t$ covers only a small range, from 17·98 to 18·11, and in Fig. 6a and b the samples define an array that roughly parallels a 143 Ma reference line. The results thus indicate that the age-corrected Pb and Nd isotope ratios are magmatic or near-magmatic values. These data reveal an overall Indian-MORB-type source (Fig. 4d–f).

The Neyriz samples display even more coherent Indian-MORB-type isotopic characteristics (Fig. 4a–c). The value of $\varepsilon_{Nd}(t)$ is nearly invariant (+7·8 to +8·2), and very little variation is present in age-corrected Pb isotope ratios, whereas present-day $^{206}Pb/^{204}Pb$ vs $^{238}U/^{204}Pb$ and $^{208}Pb/^{204}Pb$ vs $^{232}Th/^{204}Pb$ define a linear array that approximately parallels a 93 Ma reference line (Fig. 6c and d). The similar-age Samail ophiolite to the SE of Neyriz appears to have rather similar age-corrected Nd–Pb isotope characteristics, although Nd and Pb isotopes were measured on different samples (Chen & Pallister, 1981; McCulloch *et al.*, 1981).

Albania

Albania hosts two Jurassic Tethyan ophiolites. Magmatic rocks of the western ophiolite are predominantly N-MORB-type in trace and major element and mineral composition (e.g. Beccaluva *et al.*, 1994; Bortolotti *et al.*, 2002). Boninite dikes and some later arc-type lavas are also present, however, and this ophiolite has been interpreted as a section of normal oceanic lithosphere that became incorporated into a fore-arc of the western Neotethys (e.g. Bortolotti *et al.*, 2002). Radiolarians in chert atop pillow basalts have been dated as late Bajocian to early Callovian, ~165 Ma (Marucci *et al.*, 1994).

As with the broadly MORB-like Tibetan and Iranian rocks, the Albanian basalts show only a small range in $\varepsilon_{Nd}(t)$ (+7·1 to +7·8); $(^{87}Sr/^{86}Sr)_t$ again varies widely, and in one case, leaching lowered $(^{87}Sr/^{86}Sr)_t$ by 0·00132. Unlike the Tibetan and Iranian samples, the Pb isotope systematics of at least some of the Albanian rocks appear

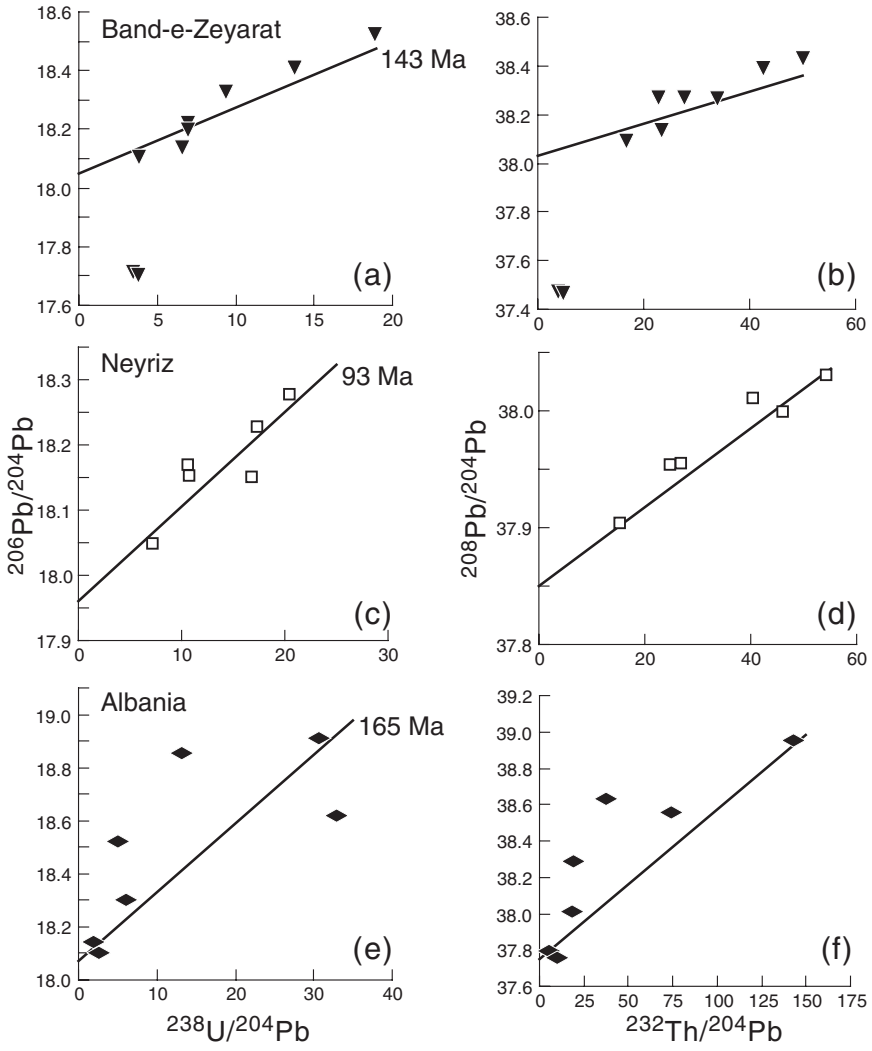

Fig. 6. Present-day $^{206}Pb/^{204}Pb$ vs $^{238}U/^{204}Pb$ and $^{208}Pb/^{204}Pb$ vs $^{232}Th/^{204}Pb$ for ophiolite samples from Band-e-Zeyarat (a, b), Neyriz (c, d), and Albania (e, f). Also plotted are 143 Ma, 93 Ma, and 165 Ma reference isochrons. Analytical errors are smaller than the size of the symbols, except for (d), in which the errors on $^{208}Pb/^{204}Pb$ are about three times the height of the symbols.

to have been disturbed significantly. The $(^{206}Pb/^{204}Pb)_t$ value varies from 17·77 to 18·51, which is a large range considering that this ophiolite covers a small area and that $\varepsilon_{Nd}(t)$ in the same samples varies by only 0·7. Also, the data do not form a trend subparallel to a 165 Ma reference line in Fig. 6e and f. Another indication of disturbance to the Pb isotope system is that one point in Fig. 4f falls slightly below or to the right of the age-adjusted Pacific–North Atlantic MORB-source field, where no MORB or OIB data are expected to lie. Not surprisingly, these rocks do not exhibit a consistently Pacific–North Atlantic- or Indian-MORB-type signature in Fig. 4d and e.

Are any of the age-corrected Pb isotope ratios representative of the original (magmatic) values? Samples AL-1 and RU-124 have (1) very low $^{238}U/^{204}Pb$ (1·94, 2·68) and $^{232}Th/^{204}Pb$ (5·35, 10·2), (2) by far the lowest present-day $^{206}Pb/^{204}Pb$ and $^{208}Pb/^{204}Pb$, and (3) very similar age-corrected Pb isotope values. Thus, the age-corrected ratios of AL-1 and RU-124 are unlikely to be either badly under- or over-corrected and are likely to be the most representative of the original values in the Albanian suite. Ratios for sample RU-143, despite a large age correction, are close to those of AL-1 and RU-124. Moreover, for the one sample for which we measured Pb isotopes in a leached aliquant, AL-2, the age-corrected values are close to those of these samples. Taken at face value, the data for AL-1, RU-124, and RU-143 are Indian-MORB-like in Fig. 4d but marginally Pacific–North Atlantic-like in Fig. 4e. Although these characteristics could mean that the far-western Jurassic Tethys was isotopically transitional, the ambiguous nature of the Pb isotope data

precludes any conclusive statement. Without reference to Pb isotopes, we can say only that the relatively low $\varepsilon_{Nd}(t)$ of the Albanian rocks is more typical of Indian N-MORB than of Pacific or North Atlantic N-MORB, and thus may weakly favor an Indian-MORB-like source.

Northwestern Australian margin

A continental block (Argo Land) rifted in the Jurassic from the portion of Gondwana that is now northwestern Australia (e.g. Audley-Charles *et al.*, 1988). Breakup was followed, slightly before 155 Ma, by seafloor spreading along a new branch of the Tethyan spreading system. At about 135 Ma, rearrangement of this system led to the formation of a new seaway between Australia and Greater India that eventually developed into the northeastern Indian Ocean (e.g. Powell *et al.*, 1988). The breakup events are recorded in extensive volcanic sequences along the northwestern margin of Australia. Farther offshore, a sizeable remnant of the post-breakup Tethyan Ocean crust is preserved in the Argo Abyssal Basin.

Dredge samples

Breakup-related lavas were dredged along the lower slopes of the Australian margin (Fig. 1) during cruises 95 and 96 of the *Rig Seismic*. On the basis of trace and major element data, the rocks range from E-MORB to N-MORB (Crawford & von Rad, 1994). Dredge haul 95/10 recovered E-MORB of Oxfordian–Callovian age (~160 Ma). Dredges 96/08, 23, and 24 yielded slightly less incompatible-element-enriched Oxfordian–Callovian E-MORB, and dredge 96/34 contained Valanginian (~134 Ma) T- to N-MORB. We analyzed isotope ratios of eight samples from these dredges and, for five samples, measured both unleached and leached splits. Leaching again variably lowered $(^{87}Sr/^{86}Sr)_t$, whereas Pb isotope ratios and $\varepsilon_{Nd}(t)$ in the leached and unleached pairs were similar.

The E-MORB from dredges 96/23 and 96/24, on the flank of the Scott Plateau, have similar age-corrected values that fall in or near the age-adjusted Re–Cr–Am source field in Figs 4 and 5. Similar $\varepsilon_{Nd}(t)$ and $(^{206}Pb/^{204}Pb)_t$ values were obtained for the two E-MORB from dredge 95/10 on Rowley Terrace, the 95/10 rocks differing from those of 96/23 and 24 in having slightly lower $(^{207}Pb/^{204}Pb)_t$ and $(^{87}Sr/^{86}Sr)_t$.

Three T- and N-MORB-type samples from dredge 96/34 at the foot of the Exmouth Plateau have higher Nd and lower Pb isotope ratios [e.g. $\varepsilon_{Nd}(t) = +5{\cdot}8$ to $+6{\cdot}9$] than the E-MORB. Sr isotopes were measured only for unleached splits, but only modest alteration of $(^{87}Sr/^{86}Sr)_t$ is indicated by the position of the data within or close to the MORB-source field in Fig. 5. Most importantly, the 96/34 data display a consistently Indian-MORB-type signature in Fig. 4a–c.

The dredge 96/08 sample is distinct, with very high $(^{207}Pb/^{204}Pb)_t$ (15·69), low $\varepsilon_{Nd}(t)$ (+0·9), and high $(^{87}Sr/^{86}Sr)_t$ (0·70670). In combination, these characteristics suggest an influence from continental crust or lithospheric mantle. Consistent with this interpretation, the incompatible element pattern of this rifted-margin basalt, although generally E-MORB-like, shows a depletion in Nb, with $(Th/Nb)_n = 3{\cdot}3$ (Crawford & von Rad, 1994).

Drill-core samples

The Argo Abyssal Basin was drilled at DSDP Site 261 and Ocean Drilling Program (ODP) Site 765 (Shipboard Scientific Party, 1974, 1990). Site 765 is on Tethyan crust with a magnetic (chron M26) and radiometric age of ~155 Ma (Ludden, 1992), whereas Site 261 is on ~152 Ma (chron M24A) crust. At Site 261, a 10 m thick basalt sill and two lava units were cored. At Site 765, two basalt units were identified in Hole 765C, and about 30 m away, 22 units in Hole 765D. All of these rocks are chemically N-MORB (Robinson & Whitford, 1974; Ludden & Dionne, 1992; Weis & Frey, 1996).

Ludden & Dionne (1992) measured present-day isotope ratios of several Site 765 basalts. For Site 261, a sample from the sill and one from the upper lava unit were analyzed by Weis & Frey (1996), yielding $\varepsilon_{Nd}(t)$ of +11·1 and +14·5, respectively, and $(^{206}Pb/^{204}Pb)_t$ of 17·72 and 17·89. This combination of values lies in or to the high-$\varepsilon_{Nd}(t)$ side of the Pacific–North Atlantic MORB-source field in Fig. 4d. However, $^{143}Nd/^{144}Nd$ was measured on leached splits, whereas Sm and Nd concentrations used for the age correction were determined on unleached splits. Because leaching preferentially removes more-soluble minerals, Sm/Nd can be significantly different in leached splits than in unleached splits [e.g. see data for 261-35R-4 (98–100) in Table 1]; therefore this approach can result in under- or over-correction of $\varepsilon_{Nd}(t)$. Age-corrected $(^{208}Pb/^{204}Pb)_t$ was not reported, but $(^{207}Pb/^{204}Pb)_t$ was higher, at 15·50 and 15·59, than for Pacific–North Atlantic MORB mantle at the same $(^{206}Pb/^{204}Pb)_t$; the 15·59 value is also higher than for Indian MORB mantle. Weis & Frey (1996) suspected that such high $(^{207}Pb/^{204}Pb)_t$ values were caused by small amounts of sample contamination by Pb derived from marine sediment.

We measured four samples from Site 261, two from the upper and lower parts of the sill and one from each lava unit, plus one sample each from Holes 765C and 765D. All have closely similar $\varepsilon_{Nd}(t)$, between +8·3 and +8·8. The range of $(^{87}Sr/^{86}Sr)_t$ is also relatively small (0·70288–0·70323; Fig. 5), and $(^{207}Pb/^{204}Pb)_t$ is between 15·42 and 15·48, with one exception (see below). Again with one exception, the age-corrected Nd and Pb isotope ratios plot within the Indian MORB mantle field (or in one case slightly to the left of it in Fig. 4d and e).

Although Indian-MORB-like, the range of $(^{206}Pb/^{204}Pb)_t$ is substantial, from 17·05 to 17·86 for the unleached splits. This spread of $(^{206}Pb/^{204}Pb)_t$ at nearly constant $\varepsilon_{Nd}(t)$ strongly suggests that the Pb isotope systematics of some of the samples are disturbed. Not surprisingly, the data are scattered about a 155 Ma reference line in a $^{206}Pb/^{204}Pb$ vs $^{238}U/^{204}Pb$ diagram (not shown). Most suspect are samples whose Pb isotope ratios are the most sensitive to even minor disturbance; that is, those with large parent–daughter ratios, for which the age correction is greatest. These are the Site 765C basalt and sample 35R-4 (98–100) from the upper lava unit of Site 261, which have very high $^{238}U/^{204}Pb$ (110 and 108). The Site 765C sample has by far the lowest age-corrected $(^{206}Pb/^{204}Pb)_t$, its data point actually falling outside (to the left of) the Indian MORB-source field in Fig. 4d and e. Also, we leached a split of 35R-4 (98–100), and the age-corrected $(^{206}Pb/^{204}Pb)_t$ and $(^{207}Pb/^{204}Pb)_t$ values for the two splits are drastically different (17·60 and 15·49 vs 19·89 and 15·62), the data for the leached split plotting far out to the right of Pacific–North Atlantic MORB-source array in Fig. 4d–f.

In contrast, the leached and unleached splits of the sill sample that we leached [35R-2 (87–89)] have almost identical values (17·34, 15·45 and 17·34, 15·44), which are also similar to those of the other (unleached) sill sample (17·44, 15·45). These results suggest that the data for the sill represent near-magmatic values despite a significant age correction. Likewise, almost identical $(^{206}Pb/^{204}Pb)_t$ and $(^{207}Pb/^{204}Pb)_t$ were obtained for the leached (17·86, 15·48) and unleached (17·83, 15·47) splits of the lower lava unit of Site 261. For this sample and the Hole 765D basalt, which has very similar values (17·81, 15·46), the age correction is relatively small, as $^{238}U/^{204}Pb$ is relatively low (12·7–15·0). The age-corrected Pb isotope values for these samples too are likely to be near-magmatic.

Eastern Himalayan syntaxis

In China, Burma, and extreme northeastern India, fragments of Paleotethyan lithosphere ranging from Early Carboniferous to Permian are exposed in several ophiolite zones (Fig. 1) in which the magmatic rocks predominantly have N-, T-, or E-MORB-type trace and major element compositions (e.g. Mo *et al.*, 1993, 1994, 1998; Wu *et al.*, 1995; Shen *et al.*, 2002*a*, 2002*b*; Ghosh & Ray, 2003). Xu & Castillo (2004) analyzed N-MORB-type gabbro of the Early Carboniferous Shuanggou ophiolite in the Ailaoshan ophiolite zone of southwestern China, and Early Permian T-MORB-type basalt from two sites in the Jinsha River ophiolite north of the Ailaoshan zone. Their data suggest sources with broadly Indian-MORB-like Nd–Pb isotopic characteristics but, like our results for the Albanian and Site 261 and 765 basalts, and those of Xu *et al.* (2002) for the Carboniferous northern Mian–Lue ophiolite of central China, the data do not consistently all fall inside the Indian MORB-source field in Fig. 7.

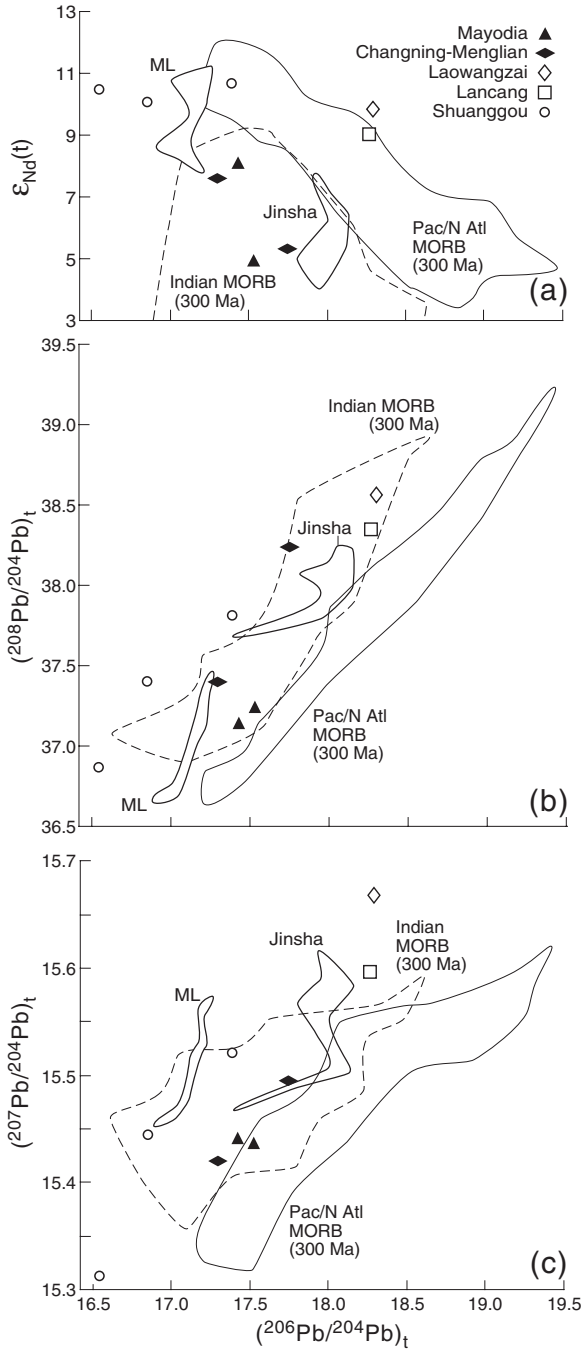

Fig. 7. Age-corrected $\varepsilon_{Nd}(t)$ (a), $(^{208}Pb/^{204}Pb)_t$ (b), and $(^{207}Pb/^{204}Pb)_t$ (c) vs $(^{206}Pb/^{204}Pb)_t$ for Paleotethyan ophiolites compared with estimated 300 Ma fields for Pacific–North Atlantic and Indian MORB mantle. The ML field is for the Mian–Lue northern ophiolite samples of Xu *et al.* (2002); the Jinsha (River) ophiolite field and data for gabbros of the Shuanggou ophiolite are from Xu & Castillo (2004).

Here, we report isotopic results for six Paleotethyan basalts: two each from the Early Carboniferous Changning–Menglian ophiolite of southwestern China and the Permian Mayodia ophiolite of northeastern India, and one sample each from the Early Carboniferous Laowangzai area of the Ailaoshan ophiolite and the Early Permian Lancang River zone of southwestern China. Alteration-resistant trace and major elements indicate N-MORB-type compositions for all (Mo *et al.*, 1998; Shen *et al.*, 2002*a*, 2002*b*; Ghosh & Ray, 2003).

Two samples, LZK1-3 from Laowangzai and HN-4 from the Lancang River zone, are isotopically unlike either Indian or Pacific–North Atlantic MORB, the data falling at the upper edge of the estimated 300 Ma Pacific–North Atlantic MORB-source field in Fig. 7a, within the Indian MORB-source field in Fig. 7b, and above both fields in Fig. 7c. We infer that these rocks contain some Pb derived from continental material or marine sediment, probably an overprint introduced during hydrothermal alteration or ophiolite obduction. Further evidence of such an overprint is seen in their high $(^{87}Sr/^{86}Sr)_t$ (0·70984, 0·70585), the value for LZK1-3 being greater than Carboniferous-to-present seawater values (e.g. Burke *et al.*, 1982).

In contrast, the samples from the Changning–Menglian and Mayodia ophiolites all exhibit consistently Indian MORB-type Pb–Pb and Nd–Pb isotope signatures; $(^{206}Pb/^{204}Pb)_t$ is relatively low for their $\varepsilon_{Nd}(t)$ and $(^{208}Pb/^{204}Pb)_t$ and, importantly, $(^{207}Pb/^{204}Pb)_t$ is not anomalously high but well within the Indian MORB-source field in Fig. 7c. These basalts also have much lower $(^{87}Sr/^{86}Sr)_t$ for their $\varepsilon_{Nd}(t)$ than LZK1-3 and HN-4.

DISCUSSION

A widespread Indian-Ocean-type isotopic signature in the Tethyan mantle

Rocks from two locations in Iran, a 1300 km stretch of Tibet, and off northwestern Australia demonstrate that mantle sources very similar to those feeding the Indian Ocean spreading centers and hotspots today were present in a wide region of the Neotethys (Fig. 8) in the Early Cretaceous and Jurassic. The Jurassic rocks, in particular, indicate that such mantle existed in much of the central and eastern Neotethyan region before and during the earliest stages of Indian Ocean opening. Whether Indian-Ocean-like mantle also underlay the Jurassic western Neotethys is unclear; the Albanian data certainly do not rule out this possibility, and samples from the Troodos ophiolite of Cyprus, SE of and about 60 Myr younger than the Albanian ophiolite, possess broadly Indian-MORB-type Nd–Pb isotope characteristics (Xu & Castillo, 2004). Farther east, the only Jurassic or Early Cretaceous rocks studied to date that lack an Indian-Ocean-like signature are the 150 Ma N- and T-MORB suite from Masirah (Mahoney *et al.*, 1998), the crust of which was formed near the southern boundary of the Tethyan Ocean in a setting similar to that of the Gulf of Sheba today.

We emphasize that although some of the MORB-like Tethyan rocks may have been formed in intra-oceanic back-arc or even fore-arc environments rather than at mid-ocean ridges (see above), contamination of asthenosphere with marine sedimentary material subducted shortly before (or even a few hundred million years before; see Moores *et al.*, 2000) volcanism cannot be a general explanation for their Indian-Ocean-type characteristics, particularly their low relative $^{206}Pb/^{204}Pb$. Marine sediments in general have high $^{207}Pb/^{204}Pb$, $^{208}Pb/^{204}Pb$, and $^{87}Sr/^{86}Sr$ and low ε_{Nd} relative to Pacific–North Atlantic MORB, but they also have rather high $^{206}Pb/^{204}Pb$ (e.g. Ben Othman *et al.*, 1989). Sediment entering subduction zones today has average $^{206}Pb/^{204}Pb = 18{\cdot}91$ (Plank & Langmuir, 1998), and this value would have been only about 0·8 lower at the beginning of the Phanerozoic (e.g. Stacey & Kramers, 1975).

The picture that emerges is thus that the Jurassic and Early Cretaceous mantle of the central and eastern Neotethyan Ocean was isotopically equivalent to Indian Ocean mantle, except for (very?) rare pockets or stringers of broadly Pacific–North Atlantic-like composition. In contrast, the sources of all pre-120 Ma Pacific MORB yet analyzed were isotopically indistinguishable from those of modern Pacific MORB (Janney & Castillo, 1996, 1997; Mahoney *et al.*, 1998, 2004). One possibility is that both Indian Ocean and Tethyan mantle were physically separate domains but acquired similar isotopic characteristics as a result of the same process(es). However, given that the two basins were interconnected throughout the period of growth of the Indian Ocean, the most straightforward interpretation is that the present Indian Ocean domain is inherited from the Tethyan mantle domain; that is, that the crust of both oceans was derived from the same extensive region of mantle. Furthermore, although the Paleotethyan rocks provide somewhat mixed signals, the majority of results support an isotopically Indian MORB-type mantle beneath at least parts of the Paleotethyan Ocean as long ago as the Early Carboniferous (Fig. 7 and Xu *et al.*, 2002; Xu & Castillo, 2004).

Intriguingly, the Jurassic E-MORB from the Australian margin and the Early Cretaceous OIB-type rocks at Dajiweng and Bar in Tibet are isotopically similar to the recent Indian OIB of Réunion, Mauritius, Crozet, and Amsterdam. So too are Early Cretaceous ($\sim$120 Ma) OIB-type lavas at Masirah (Fig. 4a–c) (Mahoney *et al.*, 1998). Thus, hotspot-like mantle with a broadly Réunion-type isotopic composition appears to have been rather common in the Jurassic and Early Cretaceous, just as it is in far-flung parts of the Indian Ocean today.

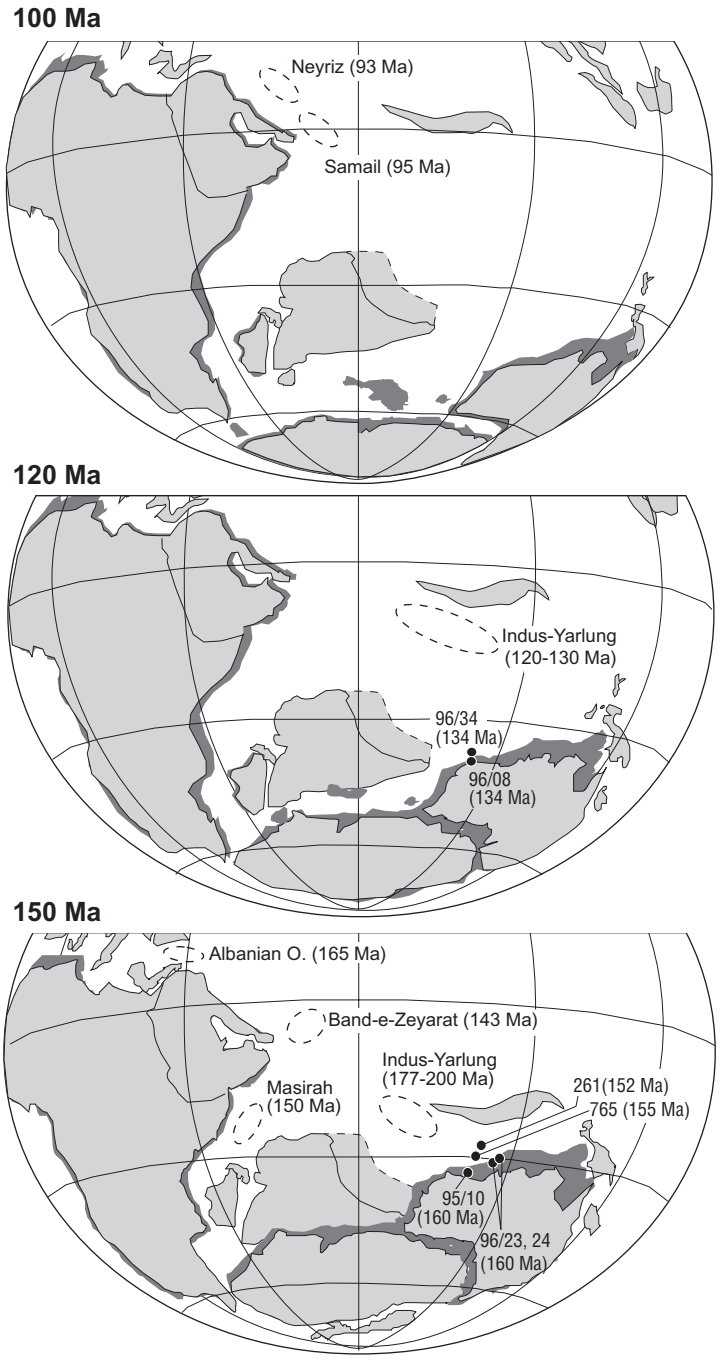

Fig. 8. Reconstructions of the Tethyan region at 100, 120, and 150 Ma (Lawver *et al.*, 2000) showing approximate original locations (dashed ellipses and black dots) of Neotethyan crust represented by samples of this study, and of that preserved in the Samail and Masirah ophiolites.

Origin of the Indian and Tethyan MORB mantle domain

The Indian MORB mantle domain is commonly suggested to be a result of addition of low-$^{206}Pb/^{204}Pb$, low-ε_{Nd}, high-$^{87}Sr/^{86}Sr$ material to the asthenosphere. This material is often postulated to be derived from (1) anciently subducted (>1 Ga), low-U/Pb marine sediments (plus a basaltic slab component, usually) (e.g. Dupré & Allègre, 1983; Hamelin *et al.*, 1986; Michard *et al.*, 1986; Price *et al.*, 1986; le Roex *et al.*, 1989; Rehkämper & Hofmann, 1997; Chauvel & Blichert-Toft, 2001), or (2) mobilization of old low-U/Pb

continental lithospheric mantle and/or lower crust during ancient continental collisions, impingement of plume heads beneath Gondwana, Gondwanan or pre-Gondwanan rifting events, and/or subduction erosion (e.g. McKenzie & O'Nions, 1983; Mahoney *et al.*, 1989, 1992; Tatsumoto & Nakamura, 1991; Douglass *et al.*, 1999; Flower *et al.*, 2001; le Roux *et al.*, 2002; Escrig *et al.*, 2004; Hanan *et al.*, 2004). A combination of (1) and (2) also has been proposed (le Roux *et al.*, 2002). In contrast, evolution of an extensive asthenospheric region isolated from plume input and from mixing with the rest of the asthenosphere since early in Earth history has been suggested (e.g. Dosso *et al.*, 1988; Xu *et al.*, 2002).

With regard to mobilization of continental lithosphere, it is noteworthy that both the Neotethys and Paleotethys largely grew by repeated rifting of portions of the supercontinent of Gondwana (e.g. Stampfli & Borel, 2002), and that large volumes of Gondwanan lower crust and lithospheric mantle indeed appear to be missing today, presumably removed at various times by one or more of the above mechanisms (e.g. Ballard & Pollack, 1988; Ashwal & Burke, 1989; Black & Liegeois, 1993; Poudjom Djomani *et al.*, 2001; Zheng *et al.*, 2001; Gao *et al.*, 2002). Regarding hypotheses involving sediment recycling, ancient marine sediments theoretically could have been introduced into the asthenosphere in three ways: they could have been mixed in directly, the hybrid mantle then evolving isotopically over >1 Gyr; they could have been subducted deeply (660 km or deeper), stored for long periods, and returned relatively recently to the upper mantle, probably by plumes; or they could have been accreted to the continental lithosphere (e.g. Von Huene & Scholl, 1991) and stored for long periods in isolation from the convecting mantle prior to entry into the asthenosphere.

The last possibility removes the distinction between sediment-recycling and continental lithosphere-mobilization hypotheses. The alternative idea that large amounts of low-$^{206}Pb/^{204}Pb$ material (whether of sedimentary origin or not) have been introduced to the asthenosphere via mantle plumes is not supported as a general explanation for Indian and Tethyan MORB mantle by either present-day Indian Ocean hotspots (e.g. Mahoney *et al.*, 1992) or by the OIB- or E-MORB-like Tethyan rocks, all of which lack sufficiently low $^{206}Pb/^{204}Pb$ (see Fig. 4). On the other hand, ancient mixing of sediments directly into the asthenosphere requires that the resulting hybrid mantle remain isolated from the rest of the asthenosphere for a very long time (>1 Gyr). For as much as a few hundred million years, isolation might be accomplished by slab 'curtains' at long-lived subduction zones, such as those that appear to have surrounded much of the Tethys and Gondwana from the Middle Paleozoic to Mesozoic (e.g. Stampfli & Borel, 2002). However, given the complexity of plate motions and ever-changing plate boundaries, isolation of any large region of asthenosphere by slab curtains for much longer times seems implausible. Indeed, the problem of maintaining convective isolation is a major challenge to any hypothesis involving a truly ancient origin for Indian and Tethyan MORB asthenosphere.

Rehkämper & Hofmann (1997) estimated that <10 wt % of contamination of (originally) Pacific–North Atlantic-type asthenosphere by 1·5 Ga subducted slab material containing <10 wt % of marine sediment could account for much of the isotopic variation in Indian MORB. For the Indian MORB domain as a whole, they estimated that the amount of subducted sediment required would be significantly less than the amount of mobilized ex-continental lithosphere (mantle only, not crust) needed to achieve the same results. For their model sediment, they assumed much higher concentrations of Pb (55 ppm) and several other elements than in average subducting marine sediment (Pb 19·9 ppm; Plank & Langmuir, 1998); thus, their estimate of the amount of sediment contamination required is best viewed as a minimum. More importantly, recent work shows that profound chemical changes occur during dehydration of sediment and basaltic crust in subduction zones. Large proportions of several trace elements, particularly Pb, are removed with the fluid phase during this process (e.g. Kogiso *et al.*, 1997; Aizawa *et al.*, 1999; Johnson & Plank, 1999; Becker *et al.*, 2000). Uranium (and Th) appears to be much less mobile than Pb during dehydration, causing $^{238}U/^{204}Pb$ in the residue of both sediment and basalt to increase significantly, probably by factors of 3–5. Therefore, unlike non-dehydrated marine sediment (which has low $^{238}U/^{204}Pb$ averaging around 4–6; Ben Othman *et al.*, 1989; Plank & Langmuir, 1998), $^{206}Pb/^{204}Pb$ in subducted, dehydrated sediment should increase rather rapidly to values higher than found in any modern MORB (and the increase will be even more rapid in dehydrated ocean crust). Aizawa *et al.* (1999), for example, estimated that $^{206}Pb/^{204}Pb$ would increase by about 2·2 per Gyr in average dehydrated, subducted marine sediment. Thus, we conclude that normal, anciently subducted marine sediment cannot be the low-$^{206}Pb/^{204}Pb$ material in the Tethyan and Indian Ocean asthenosphere. Moreover, admixture of small amounts of un-dehydrated sediment plus altered ocean crust into MORB-source mantle produces incompatible-element patterns with pronounced Pb peaks that are lacking in Indian MORB (Fig. 9a).

Relatively recent addition of low-$^{206}Pb/^{204}Pb$ lower mantle to the Indian Ocean asthenosphere, either via plumes or by a general upward 'leakage', has been suggested by Kamber & Collerson (1999). In this view, the lower mantle does not contain significant amounts of subducted material but has evolved largely in isolation

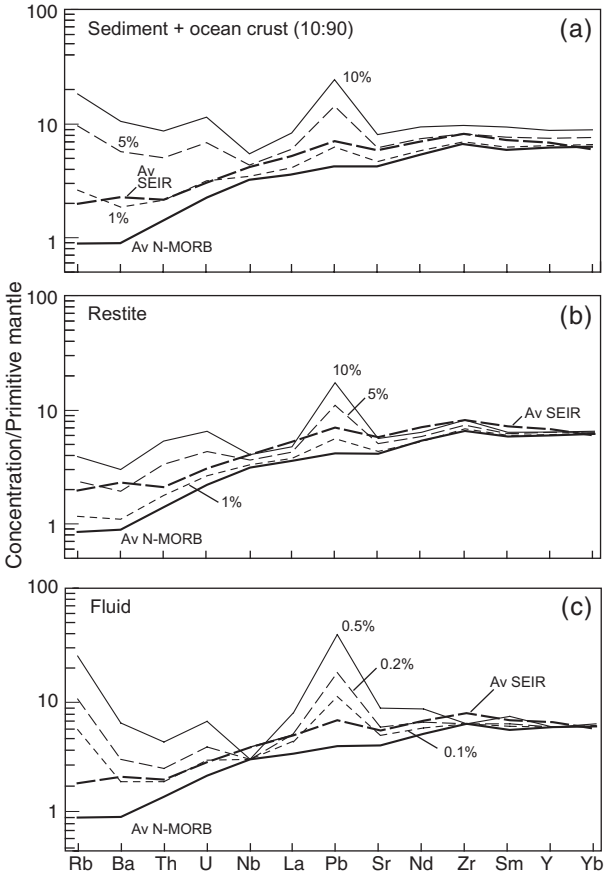

Fig. 9. Incompatible-element patterns of model basalt produced by 15% fractional melting of average MORB-source mantle that has been contaminated by variable weight percentages of (a) un-dehydrated marine sediment plus ocean crust (assumed to be in a 10:90 proportion), (b) pyroxenitic lower-crustal restite, and (c) slab-derived fluid. (See Table 4 for compositions and references.) In (c), the percentage of the fluid derived from sediment is assumed to be 10%, with 90% being from altered oceanic crust. Shown for comparison are patterns of average Southeast Indian Ridge (SEIR) N-MORB (Mahoney *et al.*, 2002; D. Christie *et al.*, unpublished data, 2000) and worldwide average N-MORB (Sun & McDonough, 1989).

from the rest of the mantle for at least 3 Gyr and is only slightly modified from a primitive composition. A similar origin has been explored for the source of the world's largest oceanic plateau, the Ontong Java in the Pacific (Tejada *et al.*, 2004). A serious problem with this hypothesis for explaining the Indian MORB domain is that it predicts that the lower mantle is only slightly degassed and has very high $^{3}He/^{4}He$ ($\sim$90 times the atmospheric ratio). Thus, Indian MORB should have higher $^{3}He/^{4}He$ than other MORB. However, $^{3}He/^{4}He$ values of Indian MORB are not higher than for MORB globally; rather, the longest hotspot-free sections of the Indian Ocean ridge system have lower than average values (Graham *et al.*, 1999; Mahoney *et al.*, 2002; Georgen *et al.*, 2003).

We suggest that other voluminous, potential low-$^{206}Pb/^{204}Pb$, sources are the pyroxenitic lower-crustal restite formed in ancient arcs by extraction of andesitic magma and/or the primary, basaltic lower crust formed in such arcs prior to andesitic magmatism. For example, Tatsumi (2000) estimated the composition of Archean pyroxenitic restite generated by melting of basaltic lower-arc crust to produce andesite (e.g. Kay & Kay, 1988; Turcotte, 1989), and showed that restite retaining a few percent of frozen andesitic melt would evolve isotopically to a low-$^{206}Pb/^{204}Pb$, low-ε_{Nd}, relatively high-$^{87}Sr/^{86}Sr$ composition similar to that found today in the Pitcairn, Hawaiian, and other EM-1-type hotspots. He argued that because of its high density, ancient restite, once detached from the lithosphere, would tend to sink deep into the lower mantle, re-emerging in Late Phanerozoic plumes to produce low-$^{206}Pb/^{204}Pb$ OIB. As noted above, the lack of low $^{206}Pb/^{204}Pb$ in Indian Ocean islands or the Tethyan OIB- and E-MORB-type rocks suggests that plume-driven contamination is not the source of low-$^{206}Pb/^{204}Pb$ Indian and Tethyan MORB-type compositions. We suggest that alternative mechanisms involving restite might be (1) long-term storage in the largely arc-generated continental lithosphere, followed by eventual detachment and mixing into the asthenosphere, (2) storage of detached restite in a zone of neutral buoyancy in the mantle Transition Zone around 660 km (e.g. Yasuda *et al.*, 1997), or (3) relatively ancient mixing of detached restite into convecting MORB-source mantle, followed by isotopic evolution of the hybrid asthenosphere. Long-term lithospheric storage avoids the need for prolonged convective isolation of a large region of asthenosphere; the same may or may not be true of storage in the Transition Zone, depending on the amount of convective coupling between it and the upper mantle. In the case of lithospheric storage, assuming sufficient amounts of ancient restite are in fact preserved in the continents, detachment presumably would occur at different times during plume-head, continental collision, and/or extension events (e.g. Meissner & Mooney, 1998; Jull & Kelemen, 2001).

Our simple mass-balance modeling using a lower-crustal restite consisting of pyroxenite plus 5 wt % retained andesite (Table 4) suggests that $<$10 wt % of contamination of Pacific–North Atlantic-type asthenosphere by 1–3 Ga restite can account for most low-$^{206}Pb/^{204}Pb$ Indian MORB (Fig. 10a–c). The great majority of Indian MORB $^{206}Pb/^{204}Pb$, $^{207}Pb/^{204}Pb$, $^{143}Nd/^{144}Nd$, and $^{87}Sr/^{86}Sr$ values can be explained by mixtures involving $<$3 wt % of a restite component. Although Fig. 10 illustrates a case involving mixing between ancient restite and average modern Pacific–North Atlantic MORB mantle, such mixing would actually involve MORB mantle with a range of isotopic compositions; also, this type of model

Table 4. Elemental concentrations (ppm) of model end-members

	Pyroxenite[1]	Restite[1] (pyroxenite +5% andesite[2])	Average N-MORB[3]	Average N-MORB source	Average altered N-MORB crust[4]	Average fluid from subducted basaltic crust[5]	Global subducting sediment[6]	Average fluid from subducted sediments[7]
Rb	0·019	2·9	0·56	0·084	12	508	57·2	113
Ba	3·2	23	6·3	0·95	26	931	776	3817
Th	0·30	0·56	0·12	0·019	0·27	7·00	6·91	17·1
U	0·086	0·15	0·047	0·0071	0·14	2·71	1·68	4·15
Nb	0·90	1·4	2·3	0·35	2	0	8·94	0
La	0·74	1·6	2·5	0·38	2·5	94·4	28·8	71·1
Pb	0·95	1·5	0·30	0·045	0·2	11·4	19·9	654
Sr	49	63	90	14	110	3071	327	2249
Nd	2·9	3·8	7·3	1·1	7·3	151	27	66·7
Zr	49	53	74	14	74	0	130	0
Sm	0·86	1·0	2·6	0·42	2·6	26·5	5·78	14·3
Y	6·9	7·5	28	5·5	28	0	29·8	0
Yb	0·62	0·69	3·1	0·61	3·1	5·13	2·76	6·82

[1]Tatsumi (2000).
[2]Rudnick & Fountain (1995).
[3]Sun & McDonough (1989).
[4]McCulloch & Gamble (1991), except that Pb is estimated assuming 35% loss from average N-MORB during alteration (see Rehkämper &Hofmann, 1997).
[5]Kogiso *et al*. (1997).
[6]Plank & Langmuir (1998).
[7]Aizawa *et al*. (1999). Composition of fluid from subducted sediments is calculated using Aizawa *et al*.'s (1999) 900°C mobility factors; that from subducted basaltic crust uses Kogiso *et al*.'s (1997) mobility factors. The andesite component in the restite is assumed to be equivalent to average continental crust in the above elements (Rudnick & Fountain, 1995). Parent–daughter ratios used in constructing Figs 9 and 11 are calculated according to the above elemental compositions except that $^{238}U/^{204}Pb$ (4·0) and $^{232}Th/^{204}Pb$ (30) for global subducting sediment are the average marine sediment values of Ben Othman *et al*. (1989), and $^{87}Rb/^{86}Sr$ (0·61) and $^{147}Sm/^{144}Nd$ (0·13) are from Rehkämper & Hofmann (1997). Average N-MORB-source concentrations are calculated assuming average N-MORB forms by 15% fractional melting (Shaw, 1970) of peridotite composed of 50% olivine, 30% orthopyroxene, and 20% clinopyroxene; crystal–liquid partition coefficients used are from the compilation of Tatsumi (2000).

does not place strong bounds on when mixing occurs. Figure 9b shows that addition of 1–5 wt % of restite to average Pacific MORB-source mantle yields basalts with incompatible element concentrations in the general range of those for average Indian MORB, but that sizeable Pb peaks are again generated. Further, restite with the Th/U composition used in Table 4 is not completely successful in accounting for the high relative $^{208}Pb/^{204}Pb$ of many Indian MORB (Fig. 10d). Also, a total restite volume of $\sim 4 \times 10^8$ km^3 would be required beneath the greater Indian Ocean region, assuming an average of only 1 wt % restite in a 550 km thick asthenosphere (i.e. 660 km minus the thickness of mature oceanic lithosphere). A restite-rich layer in the Transition Zone may be able to provide such a quantity (corresponding to a 2000 km × 2000 km slab 100 km thick), but continental lithosphere seems a less likely source because, even though large amounts of Gondwanan lower crust and mantle lithosphere may have been removed in the past, pyroxenitic restite probably comprises a rather small fraction of the total. Although not shown in the figures, we obtained similar results to those for pyroxenitic restite using Tatsumi's (2000) ancient primary basaltic lower-arc crust.

Consideration of slab dewatering suggests to us a different potential mechanism for generating Indian and Tethyan MORB-type compositions, through past addition to the asthenosphere of low-U/Pb fluids derived from dehydration of marine sediment and basaltic crust. Such fluids would metasomatize or react with their host asthenosphere, which would then evolve with relatively low U/Pb. Partial convective isolation might be promoted by downward transport of the hybrid asthenosphere to Transition-Zone depths (via initial viscous

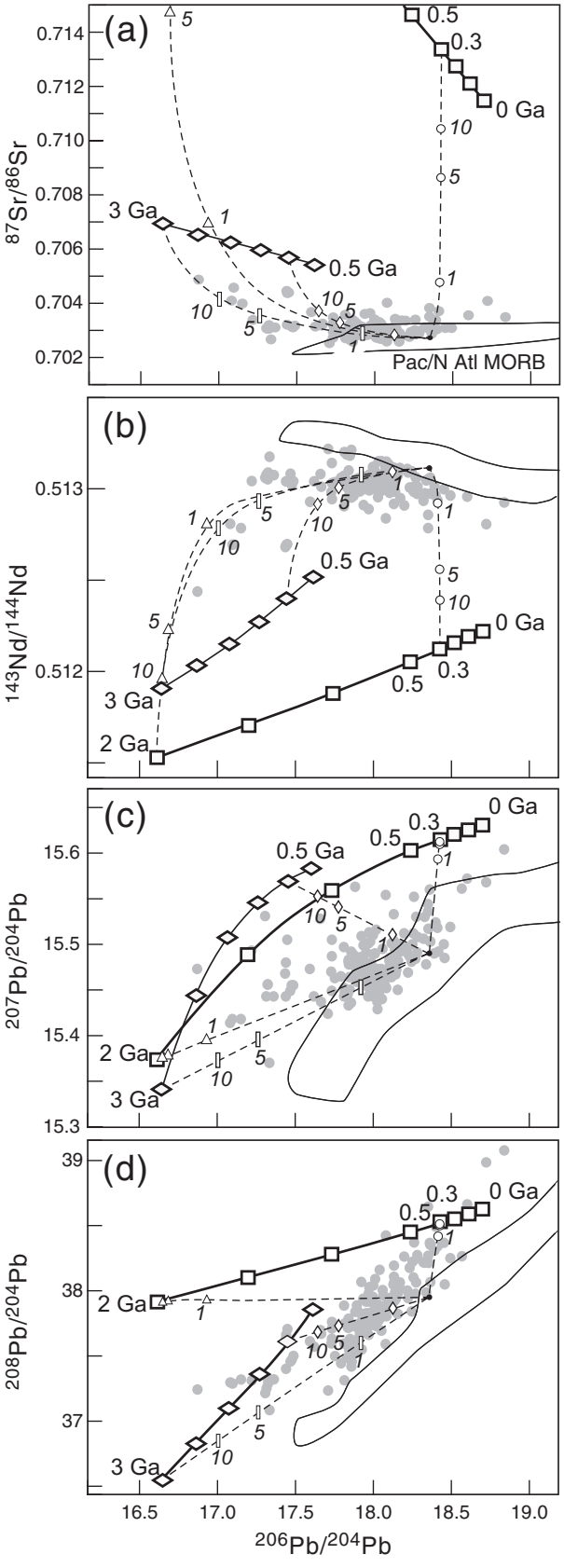

coupling to the slab; Hieronymus & Baker, 2004). Table 4 lists estimated average concentrations of several key trace elements in model fluids, calculated using Kogiso *et al.*'s (1997) and Aizawa *et al.*'s (1999) experimentally derived mobility factors and assuming the fluids are produced from average subducting sediment and altered oceanic crust. Figure 11 shows the estimated present-day isotopic ratios of hybrid asthenosphere formed at different times in the past (0·5–2 Ga) by adding 0·1, 0·2, and 0·5 wt % of slab-derived fluid to average Pacific–North Atlantic-type MORB mantle; the sediment component of the fluid is assumed to be 10% and the oceanic crust component to be 90%. Figure 11a–c shows that hybrid mantle formed at ages less than about 1·5 Ga can account for much of the isotopic range observed for Indian MORB (it also may help account for Hf–Nd isotope systematics; Kempton *et al.*, 2002). Similar to the restite example, however, the model fluid does not yield high enough present-day $^{208}Pb/^{204}Pb$ to explain a sizeable subset of the Indian MORB data (Fig. 11d). Further, the incompatible element patterns of basalts formed from model fluid-affected asthenosphere have marked Pb peaks; troughs at Nb are also evident (Fig. 9c). Thus, with the present model parameters this mechanism appears only partly successful as a means of generating Indian and Tethyan MORB mantle. Nevertheless, we feel it warrants further study, in view of the difficulties with all other proposed origins, and given that slab dewatering has been a major process throughout much of Earth history.

Fig. 10. $^{206}Pb/^{204}Pb$ vs $^{87}Sr/^{86}Sr$ (a), $^{143}Nd/^{144}Nd$ (b), $^{207}Pb/^{204}Pb$ (c), and $^{208}Pb/^{204}Pb$ (d) showing present-day isotopic composition of model lower-crustal arc restite (diamonds) formed at different times in the past between 3 and 0·5 Ga. Squares indicate present-day values for undehydrated pelagic sediment (with no accompanying ocean crust) formed at times between 2 and 0 Ga. Dashed curves illustrate mixing of mantle with average modern Pacific–North Atlantic MORB (including N-, T-, and E-MORB) isotope ratios ($^{87}Sr/^{86}Sr = 0·7027$, $^{143}Nd/^{144}Nd = 0·513115$, $^{206}Pb/^{204}Pb = 18·35$, $^{207}Pb/^{204}Pb = 15·49$, $^{208}Pb/^{204}Pb = 37·95$) with model 3 Ga and 1 Ga restite, and 2 Ga and 0·3 Ga sediment. Numbers and small symbols on curves indicate weight percentage of restite or sediment in the mixture. Sources of Indian (gray dots) and Pacific–North Atlantic MORB data are given in Fig. 4 caption. The model restite (see Table 4) is assumed to consist of 95% pyroxenite residue of andesite melting plus 5% retained andesite melt, and to evolve isotopically according to Tatsumi's (2000) model, with $^{87}Rb/^{86}Sr = 0·13$, $^{147}Sm/^{144}Nd = 0·1597$, $^{238}U/^{204}Pb = 6·3$, and $^{232}Th/^{204}Pb = 24$. The isotope ratios of the sediment at the time of subduction are calculated using a single-stage model of continental evolution for Sr and Nd isotopes, assuming $^{87}Rb/^{86}Sr = 0·186$ and $^{147}Sm/^{144}Nd = 0·183$ (Rekhämper & Hofmann, 1997), and a two-stage Stacy & Kramers (1975) model of evolution for Pb isotopes, with first-stage $^{238}U/^{204}Pb = 7·19$ and $^{232}Th/^{204}Pb = 4·62$ and second-stage $^{238}U/^{204}Pb = 9·74$ and $^{232}Th/^{204}Pb = 3·78$. The present-day isotope ratios of the subducted sediment are calculated assuming $^{87}Rb/^{86}Sr = 0·61$, $^{147}Sm/^{144}Nd = 0·13$, $^{238}U/^{204}Pb = 4$, and $^{232}Th/^{204}Pb = 30$ after Rekhämper & Hofmann (1997) and Ben Othman *et al.* (1989), and using the Pb, Nd, and Sr concentrations of average modern subducting sediment in Table 4.

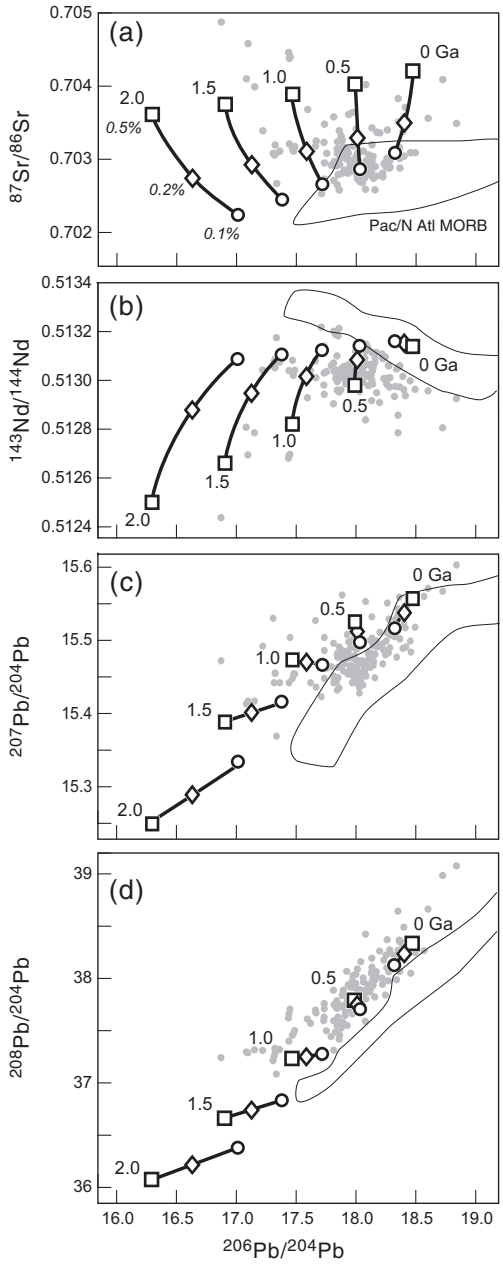

Fig. 11. $^{206}Pb/^{204}Pb$ vs $^{87}Sr/^{86}Sr$ (a), $^{143}Nd/^{144}Nd$ (b), $^{207}Pb/^{204}Pb$ (c), and $^{208}Pb/^{204}Pb$ (d) showing calculated present-day isotopic values of MORB-source mantle that was contaminated with 0·1 wt % (○), 0·2 wt % (◇), or 0·5 wt % (□) of model slab-derived fluid at different times in the past between 2 and 0 Ga (curves connect compositions of mantle contaminated at the time labeled). The proportion of the fluid derived from dehydration of marine sediment is assumed to be 10% and that from dehydration of altered basaltic crust 90% (see Table 4 for chemical compositions). Isotopic ratios of the sediment-derived component of the fluid are assumed to be equal to those of the sediment at the time of subduction (calculated as for Fig. 10); for the basalt-derived portion of the fluid, Nd and Pb isotope ratios are assumed to be those of unaltered average modern Pacific–North Atlantic MORB (see Fig. 10 caption) back-calculated to the time of subduction, whereas for $^{87}Sr/^{86}Sr$ a present-day value of 0·7055 is assumed for average altered oceanic crust (Staudigel *et al.*, 1995; Tatsumi, 2000).

CONCLUSIONS

The collective Nd–Pb and Pb–Pb isotopic data for Tethyan magmatic rocks suggest that Indian MORB mantle is largely 'inherited' from Tethyan mantle; that is, that the crust of both oceans was formed from the same mantle domain, and that the age of this domain is substantially greater than the age of the earliest Indian Ocean crust. Besides Indian-MORB-type mantle, OIB-like mantle broadly similar to that producing the widely separated modern Indian Ocean islands of Réunion, Mauritius, Crozet, and Amsterdam was also present in the Jurassic and Early Cretaceous Tethys.

In addition to previously proposed mechanisms for the origin of the Indian MORB mantle domain, two other processes that can produce basalts with a number of the key isotopic characteristics of Indian MORB are introduction of ancient pyroxenitic lower-crustal restite (or basaltic lower-arc crust) into originally Pacific–North Atlantic-type mantle, and past addition of low-U/Pb fluids derived from dewatering of subducted sediment and ocean crust to originally Pacific–North Atlantic-type mantle. At present, however, both of these processes also appear to have significant shortcomings, as do all previously proposed mechanisms.

ACKNOWLEDGEMENTS

We thank H. Babaie, L. Beccaluva, J.-Z. Li, J. Ray, S.-Y. Sheng, and Q.-W. Zhu for supplying samples, elemental data, and/or petrographic data, and K. Spencer, D. Vonderhaar, R. Carmody, S. Zhou, Badengzhu, Z. Lei, Qiongda, and N. Hulbirt for help with other aspects of the work. A. Hassanipak provided valuable field expertise in Iran. The Site 261 and 765 samples were provided by the Ocean Drilling Program. P. Janney, an anonymous referee, and P. Castillo provided insightful reviews. Principal funding came from US NSF grant EAR-9805318, Chinese NSF grants 49772107 and 49802005, and Chinese National Key Project G1998040800.

SUPPLEMENTARY DATA

Supplementary data for this paper are available at *Journal of Petrology* online.

REFERENCES

Aitchison, J. C., Badengzhu, Davis, A. M., Liu, J.-B., Luo, H., Malpas, J. G., McDermid, I. R. C., Wu, H.-Y., Ziabrev, S. V. & Zhou, M.-F. (2000). Remnants of a Cretaceous intra-oceanic subduction system within the Yarlung–Zangbo suture (southern Tibet). *Earth and Planetary Science Letters* **183**, 231–244.

Aizawa, Y., Tatsumi, Y. & Yamada, H. (1999). Element transport by dehydration of subducted sediments: implication for arc and ocean island magmatism. *Island Arc* **8**, 38–46.

Ashwal, L. D. & Burke, K. (1989). African lithospheric structure, volcanism, and topography. *Earth and Planetary Science Letters* **96**, 8–14.

Audley-Charles, M. G., Ballantyne, P. D. & Hall, R. (1988). Mesozoic–Cenozoic rift–drift sequence of Asian fragments from Gondwanaland. *Tectonophysics* **155**, 317–330.

Babaie, H. A., Ghazi, M., Babaie, A., Duncan, R., Mahoney, J. & Hassanipak, A. A. (2003). New Ar–Ar age, isotopic, and geochemical data for basalts in the Neyriz ophiolite, Iran. *Geophysical Research Abstracts, European Geophysical Society* **5**, 12899.

Ballard, S. & Pollack, H. N. (1988). Modern and ancient geotherms beneath southern Africa. *Earth and Planetary Science Letters* **88**, 132–142.

Beccaluva, L., Coltorti, M., Premti, I., Saccani, E., Siena, F. & Zeda, O. (1994). Mid-ocean ridge and suprasubduction affinities in the ophiolitic belts of Albania. *Ofioliti* **19**, 77–96.

Becker, H., Jochum, K. P. & Carlson, R. W. (2000). Trace element fractionation during dehydration of eclogites from high-pressure terranes and the implications for element fluxes in subduction zones. *Chemical Geology* **163**, 65–99.

Benoit, M. (1997). Caractérisation géochimique (traces, isotopes) d'un système de drainage magmatique fossile dans l'ophiolite d'Oman. Ph.D. thesis, Université Paul Sabatier, Toulouse, 166 pp.

Ben Othman, D., White, W. M. & Patchett, J. (1989). The geochemistry of marine sediments, island arc magma genesis, and crust–mantle recycling. *Earth and Planetary Science Letters* **94**, 1–21.

Black, R. & Liegeois, J.-P. (1993). Cratons, mobile belts, alkaline rocks and continental lithospheric mantle: the Pan-African testimony. *Journal of the Geological Society, London* **150**, 89–98.

Bortolotti, V., Marroni, M., Pandolfi, L., Principi, G. & Saccani, E. (2002). Interaction between mid-ocean ridge and subduction magmatism in Albanian ophiolites. *Journal of Geology* **110**, 561–576.

Burke, W. H., Denison, R. E., Hetherington, E. A., Koepnick, R. B., Nelson, H. F. & Otto, J. B. (1982). Variation of seawater $^{87}Sr/^{86}Sr$ throughout Phanerozoic time. *Geology* **10**, 516–519.

Castillo, P. R. (1996). Origin and geodynamic implication of Dupal isotopic anomaly in volcanic rocks from the Philippine island arcs. *Geology* **24**, 271–274.

Chauvel, C. & Blichert-Toft, J. (2001). A hafnium isotope and trace element perspective on melting of the depleted mantle. *Earth and Planetary Science Letters* **190**, 137–151.

Chen, J. & Pallister, J. S. (1981). Lead isotopic studies of the Samail ophiolite, Oman. *Journal of Geophysical Research* **86**, 2699–2708.

Coleman, R. G. (1981). Tectonic setting for ophiolite obduction in Oman. *Journal of Geophysical Research* **86**, 2699–2708.

Crawford, A. J. & von Rad, U. (1994). The petrology, geochemistry and implications of basalts dredged from the Rowley Terrace–Scott Plateau and Exmouth Plateau margins, Northwestern Australia. *AGSO Journal of Australian Geology & Geophysics* **15/1**, 43–54.

Crawford, A. J., Briqueu, L., Laporte, C. & Hasenaka, T. (1995). Coexistence of Indian and Pacific oceanic upper mantle reservoirs beneath the central New Hebrides island arc. In: Taylor, B. & Natland, J. H. (eds) *Active Marginal Basins of the Western Pacific. Geophysical Monograph, American Geophysical Union* **88**, 199–217.

Dosso, L., Bougault, H., Beuzart, P., Calvez, J.-Y. & Joron, J.-L. (1988). The geochemical structure of the South-east Indian Ridge. *Earth and Planetary Science Letters* **88**, 47–59.

Douglass, J. Schilling, J.-G. & Fontignie, D. (1999). Plume–ridge interactions of the Discovery and Shona mantle plumes with the Southern Mid-Atlantic Ridge (40°–55°S). *Journal of Geophysical Research* **104**, 2941–2962.

Duncan, R. A. (2002). A time frame for construction of the Kerguelen Plateau and Broken Ridge. *Journal of Petrology* **43**, 1109–1119.

Dupré, B. & Allègre, C. J. (1983). Pb–Sr isotope variation in Indian Ocean basalts and mixing phenomena. *Nature* **303**, 142–146.

Eggins, S. M., Woodhead, J. D., Kinsley, L. P. J., Mortimer, G. E., Sylvester, P., McCulloch, M. T., Hergt, J. M. & Handler, M. R. (1997). A simple method for the precise determination of 40 trace elements in geological samples by ICPMS using enriched isotope internal standardization. *Chemical Geology* **134**, 311–326.

Escrig, S., Capmas, F., Dupré, B. & Allègre, C. J. (2004). Osmium isotopic constraints on the nature of the DUPAL anomaly from Indian mid-ocean-ridge basalts. *Nature* **431**, 59–63.

Flower, M. F. J., Russo, R. M., Tamaki, K. & Hoang, N. (2001). Mantle contamination and the Izu–Bonin–Mariana (IBM) 'high-tide mark': evidence for mantle extrusion caused by Tethyan closure. *Tectonophysics* **333**, 9–34.

Gao, S., Rudnick, R. L., Carlson, R. W., McDonough, W. F. & Liu, Y.-S. (2002). Re–Os evidence for replacement of ancient mantle lithosphere beneath the North China craton. *Earth and Planetary Science Letters* **198**, 307–322.

Georgen, J. E., Kurz, M. D., Dick, H. J. B. & Lin, J. (2003). Low $^{3}He/^{4}He$ ratios in basalt glasses from the western Southwest Indian Ridge (10°–24°E). *Earth and Planetary Science Letters* **206**, 509–528.

Ghazi, A. M., Hassanipak, A. A., Mahoney, J. J. & Duncan, R. A. (2004). Geochemical characteristics, ^{40}Ar–^{39}Ar ages and original tectonic setting of the Band-e-Zeyarat/Dar Anar ophiolite, Makran accretionary prism, S. E. Iran. In: Flower, M. (ed.) *Tectonophysics, Special Issue* **393**, 175–196.

Ghosh, B. & Ray, J. (2003). Mineral chemistry of ophiolitic rocks of Mayodia–Hunli area, Arunachal Pradesh, north-eastern India. *Memoir, Geological Society of India* **52**, 447–471.

Girardeau, J., Mercier, J.-C. C. & Wang, X. B. (1985). Petrology of the mafic rocks of the Xigaze ophiolite, Tibet. *Contributions to Mineralogy and Petrology* **90**, 309–321.

Göpel, C., Allègre, C. J. & Xu, R. (1984). Lead isotopic study of the Xigaze ophiolite (Tibet): the problem of the relationship between magmatites (gabbros, dolerites, lavas) and tectonites (harzburgites). *Earth and Planetary Science Letters* **69**, 301–310.

Govindaraju, K. (1989). Compilation of working values and sample descriptions for 272 geostandards. *Geostandards Newsletter* **13**, 1–113.

Graham, D. W., Johnson, K. T. M., Douglas-Priebe, L. & Lupton, J. E. (1999). Hotspot–ridge interaction along the Southeast Indian Ridge near Amsterdam and St. Paul islands: helium isotope evidence. *Earth and Planetary Science Letters* **167**, 297–310.

Griselin, M. (2001). Geochemical and isotopic study of the Xigaze ophiolite massifs. Ph.D. thesis, Free University of Amsterdam, 212 pp.

Hamelin, B., Dupré, B. & Allègre, C. J. (1986). Pb–Sr–Nd isotopic data of Indian Ocean ridges: new evidence of large-scale mapping of mantle heterogeneities. *Earth and Planetary Science Letters* **76**, 288–298.

Hanan, B. B., Kingsley, R. H. & Schilling, J.-G. (1986). Pb isotope evidence from the South Atlantic for migrating ridge–hotspot interactions. *Nature* **322**, 137–144.

Hanan, B., Blichert-Toft, J., Pyle, D. & Christie, D. M. (2004). Contrasting origins of the upper mantle MORB source as revealed by Hf and Pb isotopes from the Australian–Antarctic Discordance. *Nature* **432**, 91–94.

Hart, S. R. (1988). Heterogeneous mantle domains: signatures, genesis and mixing chronologies. *Earth and Planetary Science Letters* **90**, 273–296.

Hassanipak, A. A., Ghazi, A. M. & Wampler, J. M. (1996). REE characteristics and K–Ar ages of the Band Ziarat ophiolite complex, southeastern Iran. *Canadian Journal of Earth Sciences* **33**, 1534–1542.

Hedge, C. E., Futa, K., Engel, C. G. & Fisher, R. L. (1979). Rare earth abundances and Rb–Sr systematics of basalts, gabbro, anorthosite and minor granitic rocks from the Indian Ocean ridge system, western Indian Ocean. *Contributions to Mineralogy and Petrology* **68**, 373–376.

Hickey-Vargas, R. (1998). Origin of the Indian Ocean-type isotopic signature in basalts from the Philippine Sea plate spreading center: an assessment of local versus large-scale processes. *Journal of Geophysical Research* **103**, 20963–20979.

Hickey-Vargas, R., Hergt, J. M. & Spadea, P. (1995). The Indian-Ocean-type isotopic signature in Western Pacific marginal basins: origin and significance. In: Taylor, B. & Natland, J. H. (eds) *Active Margins and Marginal Basins of the Western Pacific. Geophysical Monograph, American Geophysical Union* **88**,175–197.

Hieronymus, C. & Baker, J. (2004). Deep subduction of the mantle wedge. *Geochimica et Cosmochimica Acta* **68**, Supplement 1, 560.

Jain, J. C. & Neal, C. R. (1996). Report of the ICP-MS facility, 1993–1996. Notre Dame University Open File Report, 30 pp.

Janney, P. E. & Castillo, P. R. (1996). Basalts from the Central Pacific basin: evidence for the origin of Cretaceous igneous complexes in the Jurassic western Pacific. *Journal of Geophysical Research* **101**, 2875–2893.

Janney, P. & Castillo, P. (1997). Geochemistry of Mesozoic Pacific mid-ocean ridge basalt: constraints on melt generation and evolution of the Pacific upper mantle. *Journal of Geophysical Research* **102**, 5207–5229.

Johnson, M. C. & Plank, T. (1999). Dehydration and melting experiments constrain the fate of subducted sediments. *Geochemistry, Geophysics, Geosystems* **1**, paper number 1999GC000014.

Jull, M. & Kelemen, P. B. (2001). On the conditions for lower crustal convective instability. *Journal of Geophysical Research* **106**, 6423–6446.

Kamber, B. S. & Collerson, K. D. (1999). Origin of ocean island basalts: a new model based on lead and helium isotope systematics. *Journal of Geophysical Research* **104**, 25479–25491.

Kamenetsky, V. S., Maas, R., Sushchevskaya, N. M., Norman, M. D., Cartwright, I. & Peyve, A. A. (2001). Remnants of Gondwanan continental lithosphere in the oceanic upper mantle. *Geology* **29**, 243–246.

Kananian, A., Juteau, T., Bellon, H., Darvishzadeh, A., Sabzehi, M., Whitechurch, H. & Ricou, L.-E. (2001). The ophiolite massif of Kahnuj (western Makran, southern Iran): new geological and geochronological data. *Comptes Rendus de l'Académie des Sciences, Earth and Planetary Sciences* **332**, 543–552.

Kay, R. W. & Kay, S. M. (1988). Crustal recycling and the Aleutian arc. *Geochimica et Cosmochimica Acta* **52**, 1251–1359.

Kempton, P. D., Pearce, J. A., Barry, T. L., Fitton, J. G., Langmuir, C. & Christie, D. M. (2002). Sr–Nd–Pb–Hf isotope results from ODP Leg 187: evidence for mantle dynamics of the Australian–Antarctic Discordance and origin of the Indian MORB source. *Geochemistry, Geophysics, Geosystems* **3**, paper number 2002GC000320.

Klein, E. M., Langmuir, C. H., Zindler, A., Staudigel, H. & Hamelin, B. (1988). Isotopic evidence of a mantle convection boundary at the Australian–Antarctic Discordance. *Nature* **297**, 43–46.

Kogiso, T., Tatsumi, Y. & Nakano, S. (1997). Trace element transport during dehydration processes in the subduction oceanic crust: 1. Experiments and implications for the origin of ocean island basalts. *Earth and Planetary Science Letters* **148**, 193–205.

Lanyon, R. (1995). The Balleny plume, the Australian–Antarctic Discordance, and U–Pb zircon dating of an Antarctic mafic dyke swarm. Ph.D. thesis, University of Tasmania, Hobart, 407 pp.

Lawver, L. A. & Gahagan, L. M. (1993). Subduction zones, magmatism, and the breakup of Pangea. In: Stone, D. B. & Runcorn, K. (eds) *Flow and Creep in the Solar System: Observations, Modeling and Theory*. Dordrecht: Kluwer Academic, pp. 225–247.

Lawver, L. A., Coffin, M. F., Gahagan, L. M., Campbell, D. A. & Royer, J.-Y. (2000). Opening of the Indian Ocean. PLATES Project Report, University of Texas Institute for Geophysics, 207 pp.

le Roex, A. P., Dick, H. J. B. & Fisher, R. L. (1989). Petrology and geochemistry of MORB from 25°E to 46°E along the Southwest Indian Ridge: evidence for contrasting styles of mantle enrichment. *Journal of Petrology* **30**, 947–986.

le Roux, P. J., le Roex, A. P., Schilling, J.-G., Shimizu, N., Perkins, W. W. & Pearce, N. J. G. (2002). Mantle heterogeneity beneath the Southern Mid-Atlantic Ridge: trace element evidence for contamination of ambient asthenospheric mantle. *Earth and Planetary Science Letters* **203**, 479–498.

Ludden, J. N. (1992). Radiometric age determinations for basement from Site 765 and 766, Argo Abyssal Plain and northwestern Australian Margin. In: Gradstein, F. M., Ludden, J. N., *et al.* (eds) *Proceedings of the Ocean Drilling Program, Scientific Results, 123*. College Station, TX: Ocean Drilling Program, pp. 557–559.

Ludden, J. N. & Dionne, B. (1992). The geochemistry of oceanic crust at the onset of rifting in the Indian Ocean. In: Gradstein, F. M., Ludden, J. N., *et al.* (eds) *Proceedings of the Ocean Drilling Program, Scientific Results, 123*. College Station, TX: Ocean Drilling Program, pp. 791–799.

Mahoney, J. J., Natland, J. H., White, W. M., Poreda, R., Bloomer, S. H., Fisher, R. L. & Baxter, A. N. (1989). Isotopic and geochemical provinces of the Indian Ocean spreading centers. *Journal of Geophysical Research* **94**, 4033–4053.

Mahoney, J. J., le Roex, A. P., Peng, Z. X., Fisher, R. L. & Natland, J. H. (1992). Southwestern limit of Indian Ocean ridge mantle and the origin of low $^{206}Pb/^{204}Pb$ MORB: isotope systematics of the central Southwest Indian Ridge (17°–50° E). *Journal of Geophysical Research* **97**, 19771–19790.

Mahoney, J. J., Frei, R., Tejada, M. L. G., Mo, X.-X., Leat, P. T. & Nägler, T. F. (1998). Tracing the Indian Ocean mantle domain through time: isotope results from old west Indian, East Tethyan, and South Pacific seafloor. *Journal of Petrology* **39**, 1285–1306.

Mahoney, J. J., Graham, D. W., Christie, D. M., Johnson, K. T. M., Hall, L. S. & Vonderhaar, D. L. (2002). Between a hot spot and a cold spot: isotopic variation in the Southeast Indian Ridge asthenosphere, 86°E–118°E. *Journal of Petrology* **43**, 1155–1176.

Mahoney, J. J., Duncan, R. A., Tejada, M. L. G., Sager, W. W. & Bralower, T. J. (2004). A Jurassic–Cretaceous boundary age and MORB-type mantle source for Shatsky Rise. *Geology* (in press).

Marucci, M., Kodra, A., Pirdeni, A. & Gjata, T. (1994). Radiolarian assemblages in the Triassic and Jurassic cherts of Albania. *Ofioliti* **19**, 105–114.

McCulloch, M. T. & Gamble, J. A. (1991). Geochemical and geodynamical constraints on subduction zone magmatism. *Earth and Planetary Science Letters* **102**, 358–374.

McCulloch, M. T., Gregory, G. J., Wasserburg, G. J. & Taylor, H. P. (1981). Sm–Nd, Rb–Sr, and $^{18}O/^{16}O$ isotopic systematics in an oceanic crust section: evidence from the Samail ophiolite. *Journal of Geophysical Research* **86**, 2721–2735.

McDermid, I. R. C., Aitchison, J. C., Davis, A. M., Harrison, T. M. & Grove, M. (2002). The Zedong terrane: a Late Jurassic intra-oceanic magmatic arc within the Yarlung–Tsangpo suture zone, southeastern Tibet. *Chemical Geology* **187**, 267–277.

McKenzie, D. & O'Nions, R. K. (1983). Mantle reservoirs and ocean island basalts. *Nature* **301**, 229–301.

Meissner, R. & Mooney, W. (1998). Weakness of the lower continental crust: a condition for delamination, uplift, and escape. *Tectonophysics* **296**, 47–60.

Michard, A., Montigny, R. & Schlich, R. (1986). Geochemistry of the mantle beneath the Rodriguez Triple Junction and the South-East Indian Ridge. *Earth and Planetary Science Letters* **78**, 104–114.

Mo, X.-X., Lu, F.-X., Shen, S.-Y., Zhu, Q.-W., Hou, Z.-Q., Yang, K.-H., Deng, J.-F., Liu, X.-P. & He, C.-X. (1993). *Sanjiang Tethyan Volcanism and Related Mineralization*. Beijing: Geological Publishing House, pp. 253–267.

Mo, X.-X., Deng, J.-F. & Lu, F.-X. (1994). Volcanism and evolution of Tethys in Sanjiang area, southwestern China. *Journal of Southeast Asian Earth Sciences* **9**, 325–333.

Mo, X.-X., Shen, S.-Y., Zhu, Q.-W., Xu, T.-R., Wei, Q.-R., Tan, J., Zhang, S.-Q. & Chen, H.-L. (1998). *Volcanics–Ophiolite and Mineralization of Middle–Southern Part of Sanjiang Area of Southwestern China*. Beijing: Geological Publishing House (in Chinese with English abstract), 128 pp.

Mo, X.-X., Zhao, Z.-D., & Guo, T.-Y. (2005). *Mesozoic and Cenozoic Tectono-Magmatic Events in the Tibetan Plateau*. Guangzhou: Guangdong Science and Technology Press (in Chinese with extended English abstract), in press.

Moores, E. M., Kellogg, L. H. & Dilek, Y. (2000). Tethyan ophiolites, mantle convection, and tectonic 'historical contingency': a resolution of the 'ophiolite conundrum'. In: Dilek, Y., Moores, E. M., Elthon, D. & Nicolas, A. (eds) *Ophiolites and Oceanic Crust: New Insights from Field Studies and the Ocean Drilling Program. Geological Society of America, Special Papers* **349**, 3–12.

Mukasa, S. B., McCabe, R. & Gill, J. B. (1987). Pb isotopic compositions of volcanic rocks in the west and east Philippine island arcs: presence of the Dupal isotopic anomaly. *Earth and Planetary Science Letters* **84**, 153–164.

Nadimi, A. (2002). Mantle flow patterns at the Neyriz paleo-spreading center, Iran. *Earth and Planetary Science Letters* **203**, 93–104.

Niu, Y. & Batiza, R. (1997). Trace element evidence from seamounts for recycled oceanic crust in the Eastern Pacific mantle. *Earth and Planetary Science Letters* **148**, 471–483.

Pearce, J. A. & Deng, W. (1988). The ophiolites of the Tibetan geotraverses, Lhasa to Golmud (1985) and Lhasa to Kathmandu (1986). *Philosophical Transactions of the Royal Society of London, Series A* **327**, 215–238.

Peng, Z. X. & Mahoney, J. J. (1995). Drillhole lavas from the northwestern Deccan Traps and the evolution of Réunion hotspot mantle. *Earth and Planetary Science Letters* **134**, 169–185.

Plank, T. & Langmuir, C. H. (1998). The chemical composition of subducting sediment and its consequences for the crust and mantle. *Chemical Geology* **145**, 325–394.

Poudjom Djomani, Y. H., O'Reilly, S. Y., Griffin, W. L. & Morgan, P. (2001). The density structure of subcontinental lithosphere through time. *Earth and Planetary Science Letters* **184**, 605–621.

Powell, C. M., Roots, S. R. & Veevers, J. J. (1988). Pre-breakup continental extension in East Gondwana and the early opening of the eastern Indian Ocean. *Tectonophysics* **155**, 261–283.

Pozzi, J. P., Westphal, M., Girardeau, J., Besse, J. & Zhou, Y.-X. (1984). Paleomagnetism of the Xigaze ophiolite and flysch: latitude and direction of spreading. *Earth and Planetary Science Letters* **70**, 383–394.

Price, R. C., Kennedy, A. K., Riggs-Sneeringer, M. & Frey, F. A. (1986). Geochemistry of basalts from Indian Ocean triple junction: implications for the generation and evolution of Indian Ocean ridge basalts. *Earth and Planetary Science Letters* **78**, 379–396.

Pyle, D. G., Christie, D. M. & Mahoney, J. J. (1992). Resolving an isotope boundary within the Australian–Antarctic Discordance. *Earth and Planetary Science Letters* **112**, 161–178.

Pyle, D. G., Christie, D. M., Mahoney, J. J. & Duncan, R. A. (1995). Geochemistry and geochronology of ancient southeast Indian and southwest Pacific seafloor. *Journal of Geophysical Research* **100**, 22261–22282.

Rekhämper, M. & Hofmann, A. W. (1997). Recycled ocean crust and sediment in Indian Ocean MORB. *Earth and Planetary Science Letters* **147**, 93–106.

Robinson, P. T. & Whitford, D. J. (1974). Basalts from the eastern Indian Ocean, DSDP Leg 27. In: Veevers, J. J., Heirtzler, J. R., *et al.* (eds) *Initial Reports of the Deep Sea Drilling Project, 27*. Washington, DC: US Government Printing Office, pp. 551–559.

Rudnick, R. L. & Fountain, D. M. (1995). Nature and composition of the continental crust: a lower crust perspective. *Reviews of Geophysics* **33**, 267–309.

Sarkarinejad, K. (1994). Petrology and teconic settings of the Neyriz ophiolite, southeastern Iran. In: Ishiwatari, A., Malpas, A. & Ishizuka, H. (eds) *Proceedings of the 29th International Geological Congress, Part D*. Utrecht: VSP, pp. 221–234.

Shaw, D. M. (1970). Trace element fractionation during anatexis. *Geochimica et Cosmochimica Acta* **34**, 237–243.

Shen, S.-Y., Feng, Q.-L., Liu, B.-P. & Mo, X.-X. (2002*a*). New development in studies on MORB and OIB types of volcanic rocks in Changning–Menglian belt, Sanjiang region. *Information of Science and Technology in Geology* **21**, 17–22.

Shen S.-Y., Feng, Q.-L., Liu, B.-P. & Mo, X.-X. (2002*b*). Tectonomagmatic types of volcanic rocks in South Lancangjiang belt, Sanjiang region. *Minerals and Rocks* **22**, 66–71.

Sheth, H. C., Mahoney, J. J. & Baxter, A. N. (2003). Geochemistry of lavas from Mauritius, Indian Ocean: mantle sources and petrogenesis. *International Geology Review* **45**, 780–797.

Shipboard Scientific Party (1974). Site 261. In: Veevers, J. J., Heirtzler, J. R., *et al.* (eds) *Initial Reports of the Deep Sea Drilling Project, 27*. Washington, DC: US Government Printing Office, pp. 129–192.

Shipboard Scientific Party (1990). Site 765. In: Gradstein, F. M., Ludden, J. N., *et al.* (eds) *Proceedings of the Ocean Drilling Program, Initial Reports, 123*. College Station, TX: Ocean Drilling Program, pp. 63–268.

Sinton, J. M., Ford, L. L., Chappell, B. & McCulloch, M. T. (2003). Magma genesis and mantle heterogeneity in the Manus back-arc basin, Papua New Guinea. *Journal of Petrology* **44**, 159–195.

Spadea, P., Dantonio, M. & Thirlwall, M. (1996). Source characteristics of basement rocks from the Sulu and Celebes basins (Western Pacific): chemical and isotopic evidence. *Contributions to Mineralogy and Petrology* **123**, 159–176.

Stacey, J. S. & Kramers, J. D. (1975). Approximation of terrestrial lead isotope evolution by a two-stage model. *Earth and Planetary Science Letters* **26**, 207–221.

Stampfli, G. M. & Borel, G. D. (2002). A plate tectonic model for the Paleozoic and Mesozoic constrained by dynamic plate boundaries and restored synthetic oceanic isochrons. *Earth and Planetary Science Letters* **196**, 17–33.

Staudigel, H., Davies, G. R., Hart, S. R., Marchant, K. M. & Smith, B. M. (1995). Large-scale Sr, Nd, and O isotopic anatomy of altered oceanic crust: DSDP/ODP Sites 417/418. *Earth and Planetary Science Letters* **130**, 169–185.

Stern, R. J., Jackson, M. C., Fryer, P. & Ito, E. (1993). O, Sr, Nd and Pb isotopic composition of the Kasuga cross-chain in the Mariana arc: a new perspective on the K–*h* relationship. *Earth and Planetary Science Letters* **119**, 459–475.

Subbarao, K. V. & Hedge, C. E. (1973). $^{87}Sr/^{86}Sr$ in rocks from the Mid-Indian Ocean Ridge. *Earth and Planetary Science Letters* **18**, 223–228.

Sun, S.-S. & McDonough, W. F. (1989). Chemical and isotopic systematics of oceanic basalts: implications for mantle composition and processes. In: Saunders, A. D. & Norry, M. J. (eds) *Magmatism in the Ocean Basins. Geological Society, London, Special Publications* **42**, 313–345.

Tatsumi, Y. (2000). Continental crust formation by crustal delamination in subduction zones and complementary accumulation of the enriched mantle I component in the mantle. *Geochemistry, Geophysics, Geosystems* **1**, paper number 2000GC000094.

Tatsumoto, M. & Nakamura, Y. (1991). Dupal anomaly in the Sea of Japan: Pb, Nd and Sr isotopic variations at the eastern Eurasian continental margin. *Geochimica et Cosmochimica Acta* **55**, 3697–3708.

Tejada, M. L. G., Mahoney, J. J., Castillo, P. R., Ingle, S. P., Sheth, H. C. & Weis, D. (2004). Pin-pricking the elephant: evidence on the origin of the Ontong Java Plateau from Pb–Sr–Hf–Nd isotopic characteristics of ODP Leg 192 basalts. In: Fitton, G., Mahoney, J., Wallace, P. & Saunders, A. (eds) *Origin and Evolution of the Ontong Java Plateau. Geological Society, London, Special Publications* **229**, 133–150.

Todt, W., Cliff, R. A., Hanser, A. & Hofmann, A. W. (1996). Evaluation of a ^{202}Pb–^{205}Pb double spike for high-precision lead isotopic analyses. In: Basu, A. & Hart S. (eds) *Earth Processes: Reading the Isotopic Code. Geophysical Monograph, American Geophysical Union* **95**, 429–437.

Turcotte, D. L. (1989). Geophysical processes influencing the lower continental crust. In: Mereu, R., Mueller, S. & Fountain, D. (eds) *Properties and Processes of Earth's Lower Crust. Geophysical Monograph, American Geophysical Union* **51**, 321–329.

Volker, F., McCulloch, M. T. & Altherr, R. (1993). Submarine basalts from the Red Sea: new Pb, Sr, and Nd isotopic data. *Geophysical Research Letters* **20**, 927–930.

Von Huene, R. & Scholl, D. W. (1991). Observations at convergent margins concerning sediment subduction, subduction erosion, and the growth of continental crust. *Reviews of Geophysics* **29**, 279–316.

Weis, D. & Frey, F. A. (1996). Role of the Kerguelen plume in generating the eastern Indian ocean seafloor. *Journal of Geophysical Research* **101**, 13831–13849.

White, W. M. (1993). $^{238}U/^{204}Pb$ in MORB and open system evolution of the depleted mantle. *Earth and Planetary Science Letters* **115**, 211–226.

Wu, H.-R., Boulter, C. A., Ke, B.-J., Stow, D. A. V. & Wang, Z.-C. (1995). The Changning–Menglian suture zone: a segment of the major Cathaysian–Gondwana divide in Southeast Asia. *Tectonophysics* **242**, 267–280.

Xu, J.-F. & Castillo, P. R. (2004). Geochemical and Nd–Pb isotopic characteristics of the Tethyan asthenosphere: implications for the origin of the Indian Ocean mantle domain. In: Flower, M. (ed.) *Tectonophysics, Special Issue* **393**, 9–27.

Xu, J.-F., Castillo, P. R., Li, X.-H., Yu, X.-Y., Zhang, B.-R. & Han, Y.-W. (2002). MORB-type rocks from the Paleo-Tethyan Mian–Lueyang northern ophiolite in the Qinling Mountains, central China: implications for the source of the low $^{206}Pb/^{204}Pb$ and high $^{143}Nd/^{144}Nd$ mantle component in the Indian Ocean. *Earth and Planetary Science Letters* **198**, 323–337.

Yasuda, A., Fujii, T. & Kurita, K. (1997). A composite diapir model for extensive basaltic volcanism: magmas from subducted oceanic crust entrained within mantle plumes. *Proceedings of the Japan Academy* **73**, 201–204.

Zhang, Q. & Zhou, G.-Q. (2001). *Ophiolites of China.* Beijing: Sciences Publication House (in Chinese with English abstract), 81 pp.

Zheng, J.-P., O'Reilly, S. Y., Griffin, W. L., Lu, F.-X., Zhang, M. & Pearson, N. J. (2001). Relict refractory mantle beneath the eastern North China block: significance for lithospheric evolution. *Lithos* **57**, 43–46.

Zhou, M.-F., Robinson, P. T., Malpas, J. & Li, Z.-J. (1996). Podiform chromitites in the Luobusa ophiolite (southern Tibet): implications for melt–rock interaction and chromite segregation in the upper mantle. *Journal of Petrology* **37**, 3–21.

Zhou, S., Mo, X.-X., Mahoney, J. J., Zhang, S.-Q., Guo, T.-Y. & Zhao, Z.-D. (2002). Geochronology and Nd and Pb isotope characteristics of gabbro dikes in the Luobusha ophiolite, Tibet. *Chinese Science Bulletin* **47**, 143–145.

Ziabrev, S. V., Aitchison, J. C., Abrajevitch, A., Badengzhu, Davis, A. M. & Luo, H. (2003). Precise radiolarian age constraints on the timing of ophiolite generation and sedimentation in the Dazhuqu terrane, Yarlung–Tsangpo suture zone, Tibet. *Journal of the Geological Society, London* **160**, 591–599.